Quaternary Science Reviews 60 (2013) 76–90

Contents lists available at SciVerse ScienceDirect

Quaternary Science Reviews

journal homepage: www.elsevier.com/locate/quascirev

Age of the Fjord Stade moraines in the Disko Bugt region, western Greenland, and the 9.3 and 8.2 ka cooling events

Nicolás E. Young[a,*], Jason P. Briner[a], Dylan H. Rood[b,c], Robert C. Finkel[d], Lee B. Corbett[e,f], Paul R. Bierman[e]

[a] Department of Geology, University at Buffalo, Buffalo, NY 14260, USA
[b] Scottish Universities Environmental Research Centre (SUREC), East Kilbride G75 0QF, UK
[c] Earth Research Institute, University of California, Santa Barbara, CA 93106, USA
[d] Department of Earth and Planetary Sciences, University of California-Berkeley, Berkeley, CA, USA
[e] Department of Geology, University of Vermont, Burlington, VT 05405, USA
[f] Department of Earth Sciences, Dartmouth College, Hanover, NH 03755, USA

ARTICLE INFO

Article history:
Received 30 June 2012
Received in revised form
12 September 2012
Accepted 17 September 2012
Available online

Keywords:
Greenland Ice Sheet
Moraines
^{10}Be exposure dating
Abrupt climate change

ABSTRACT

Retreat of the western Greenland Ice Sheet during the early Holocene was interrupted by deposition of the Fjord Stade moraine system. The Fjord Stade moraine system spans several hundred kilometers of western Greenland's ice-free fringe and represents an important period in the western Greenland Ice Sheet's deglaciation history, but the origin and timing of moraine deposition remain uncertain. Here, we combine new and previously published ^{10}Be and ^{14}C ages from Disko Bugt, western Greenland to constrain the timing of Fjord Stade moraine deposition at two locations ~60 km apart. At Jakobshavn Isfjord, the northern of two study sites, we show that Jakobshavn Isbræ advanced to deposit moraines ca 9.2 and 8.2–8.0 ka. In southeastern Disko Bugt, the ice sheet deposited moraines ca 9.4–9.0 and 8.5–8.1 ka. Our ice-margin chronology indicates that the Greenland Ice Sheet in two distant regions responded in unison to early Holocene abrupt cooling 9.3 and 8.2 ka, as recorded in central Greenland ice cores. Although the timing of Fjord Stade moraine deposition was synchronous in Jakobshavn Isfjord and southeastern Disko Bugt, within uncertainties, we suggest that Jakobshavn Isbræ advanced while the southeastern Disko Bugt ice margin experienced stillstands during the 9.3 and 8.2 ka events based on regional geomorphology and the distribution of ^{10}Be ages at each location. The contrasting style of ice-margin response was likely regulated by site-specific ice-flow characteristics. Jakobshavn Isbræ's high ice flux results in an amplified ice-margin response to a climate perturbation, both warming and cooling, whereas the comparatively low-flux sector of the ice sheet in southeastern Disko Bugt experiences a more subdued response to climate perturbations. Our chronology indicates that the western Greenland Ice Sheet advanced and retreated in concert with early Holocene temperature variations, and the 9.3 and 8.2 ka events, although brief, were of sufficient duration to elicit a significant response of the western Greenland Ice Sheet.

1. Introduction

Dispersed around the Greenland Ice Sheet (GrIS) periphery, high-velocity marine-terminating outlet glaciers facilitate rapid land-to-ocean transfer of ice and account for up to ~50% of the overall mass-balance budget of the ice sheet (Pfeffer et al., 2008; van den Broeke et al., 2009). Consequently, rapid changes in outlet-glacier velocity over the last decade highlight the difficulty in extrapolating ice-sheet change into the future, and have also emphasized the dynamic nature in which the GrIS responds to climate change (Joughin et al., 2004; Rignot and Kanagaratnam, 2006; Howat et al., 2007). Reconstructions of outlet-glacier and broader GrIS change extending beyond the modern instrumental record can place important empirical constraints on the sensitivity of ice masses to temperature change and can serve as tests for geophysical ice-sheet models that are used to forecast future ice-sheet dimensions (e.g. Otto-Bliesner et al., 2006; Simpson et al., 2009).

Located in Disko Bugt, western Greenland, Jakobshavn Isbræ is the GrIS' largest outlet glacier, draining ~6.5% of the ice-sheet

* Corresponding author. Present address: Lamont-Doherty Earth Observatory, Columbia University, Palisades, NY 10964, USA.
E-mail address: nicolasy@ldeo.columbia.edu (N.E. Young).

0277-3791/$ – see front matter © 2012 Elsevier Ltd. All rights reserved.
http://dx.doi.org/10.1016/j.quascirev.2012.09.028

interior and producing ~10% of the ice sheet's total iceberg output (Figs. 1 and 2; Rignot and Kanagaratnam, 2006; Weidick and Bennike, 2007). The broader ice-sheet margin within Disko Bugt is heavily influenced by Jakobshavn Isbræ's behavior and has been an area of focus since the pioneering work of Weidick (1968) who described Disko Bugt's Holocene glacial history. Of particular interest is an extensive early Holocene moraine system dispersed not only throughout the Disko Bugt region, but also across several hundred kilometers along western Greenland's ice-free fringe (Fig. 1). These 'Fjord Stade' moraines mark early Holocene positions of the ice-sheet margin during an overall period of deglaciation. Following their original identification and description (Weidick, 1968), the generation of high-resolution ice-core records from central Greenland has fueled speculation and debate regarding the Fjord Stade moraines' relation, if any, to early Holocene abrupt climate change such as the 9.3 and 8.2 ka events (Ten Brink and Weidick, 1974; Warren and Hulton, 1990; Long and Roberts, 2002; Long et al., 2006; Weidick and Bennike, 2007; Young et al., 2011a, 2011b).

New reconstructions of western GrIS change that explicitly focus on the early Holocene period and deposition of the Fjord Stade moraine system can better assess the interaction between dynamic (i.e. decoupled from climate) and climatic controls on GrIS change. In addition, comparing ice-margin chronologies from contrasting depositional settings (i.e. marine vs. land-based) can provide additional information regarding the mechanisms driving ice-sheet change. Here, we synthesize recently published ^{10}Be ages from Jakobshavn Isfjord with new ^{10}Be (all calculated in the same manner) and ^{14}C ages not yet published from southeastern Disko Bugt, in order to re-evaluate the timing and nature of Fjord Stade moraine deposition. Using this combined dataset, we compare and contrast the ice-margin chronologies from these two localities within Disko Bugt, separated by ~60 km, to develop a precise history of western GrIS behavior between ~10 and 7 ka.

2. Deglaciation and the Fjord Stade moraine system: an overview

Disko Bugt is a large embayment located on Greenland's west-central coast situated between the present coastline and the continental shelf of Baffin Bay (Fig. 1). Between the present ice-sheet margin and the coastline exists a thin ice-free strip of land that ranges between ~20 and 50 km wide across the Disko Bugt region. Bedrock in the area is composed mainly of Precambrian orthogneiss with Paleogene basalts on Disko Island (Garde and Steenfelt, 1999). The landscape consists of ice-sculpted bedrock, erratic boulders perched on bedrock and hundreds of lakes. Dissecting Disko Bugt is the east–west oriented Jakobshavn Isfjord (~800–1000 m depth), which has tributary fjords entering from the north and south (Figs. 1 and 2).

During the Last Glacial Maximum, the GrIS covered Disko Bugt and terminated on the continental shelf (Bennike and Bjorck, 2002; Long and Roberts, 2003; Funder et al., 2011). Retreat of the GrIS from the continental shelf must have occurred prior to 10.5–10.3 cal ka BP based on ^{14}C ages from the outskirts of Disko Bugt (Fig. 1; Ingólfsson et al., 1990; Long et al., 2003; Lloyd et al., 2005). Additional minimum-limiting ^{14}C ages between 9.9 and 9.3 cal ka BP from bivalves in raised marine deposits along Disko Bugt's eastern shore indicate that the GrIS had fully retreated out of Disko Bugt and onto land by ~10 ka (Figs. 1 and 2; Weidick and Bennike, 2007). Deposition of the Fjord Stade moraines occurred between ~9.5 and ~7.7 ka and the ice sheet reached its current position by ~7–6 ka in the broader Disko Bugt region, and by ~7.3 ka at Jakobshavn Isfjord (Long and Roberts, 2002; Long et al., 2006; Weidick and Bennike, 2007; Briner et al., 2010).

Distributed between ~64° and 70° N on western Greenland (Fig. 1), the north–south trending Fjord Stade moraine system represents an important phase of the western GrIS' deglaciation history (Weidick, 1968). The Fjord Stade moraine complex is composed of the older Marrait and younger Tasiussaq moraine systems (Figs. 1 and 2; Weidick, 1968; Kelly, 1985). In the Jakobshavn Isfjord region, the Marrait moraine system was deposited contemporaneously with a marine limit of ~65–75 m asl, and the Tasiussaq moraine system is associated with a marine limit of ~40–45 m asl (Weidick, 1968; Weidick and Bennike, 2007). The difference between Marrait- and Tasiussaq-related marine limits indicates that some period of time passed between deposition of each moraine system; however, pre-existing radiocarbon control only broadly constrains deposition of the Fjord Stade moraines to ~9.5–7.7 ka (Weidick and Bennike, 2007).

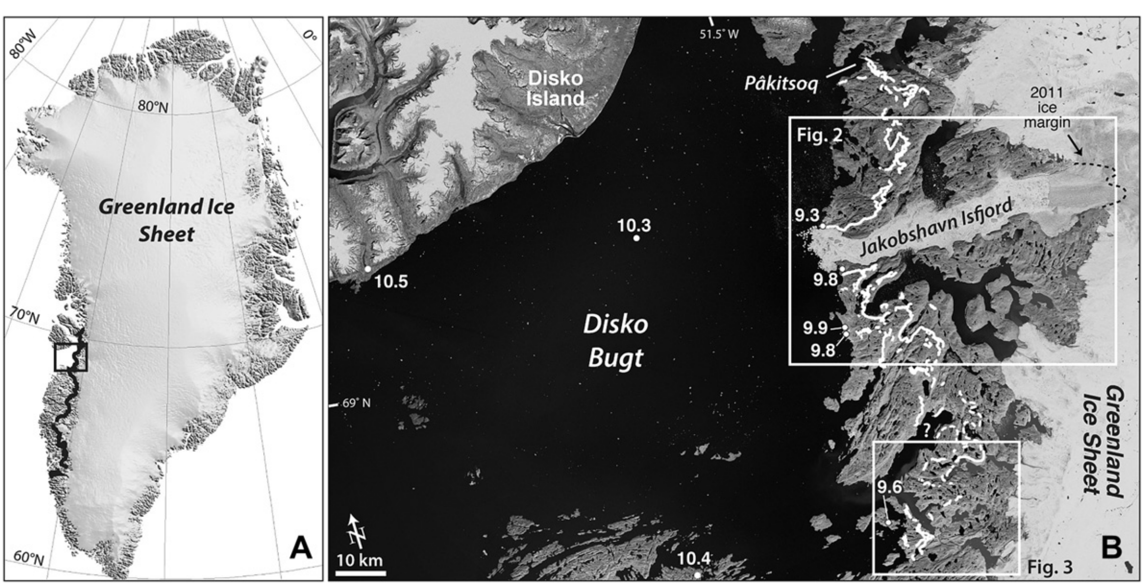

Fig. 1. (A) The Greenland Ice Sheet and the Fjord Stade moraines, western Greenland (black line; Weidick, 1968; Funder et al., 2011). (B) Disko Bugt region showing the Fjord Stade moraine complex (white lines; new mapping), and previously published ^{14}C ages (cal ka BP) that mark the timing of local deglaciation prior to Fjord Stade moraine deposition (see Table 2). Dashed lines are inferred ice limits due to poor air photo coverage. Basemap is a mosaic of Landsat imagery.

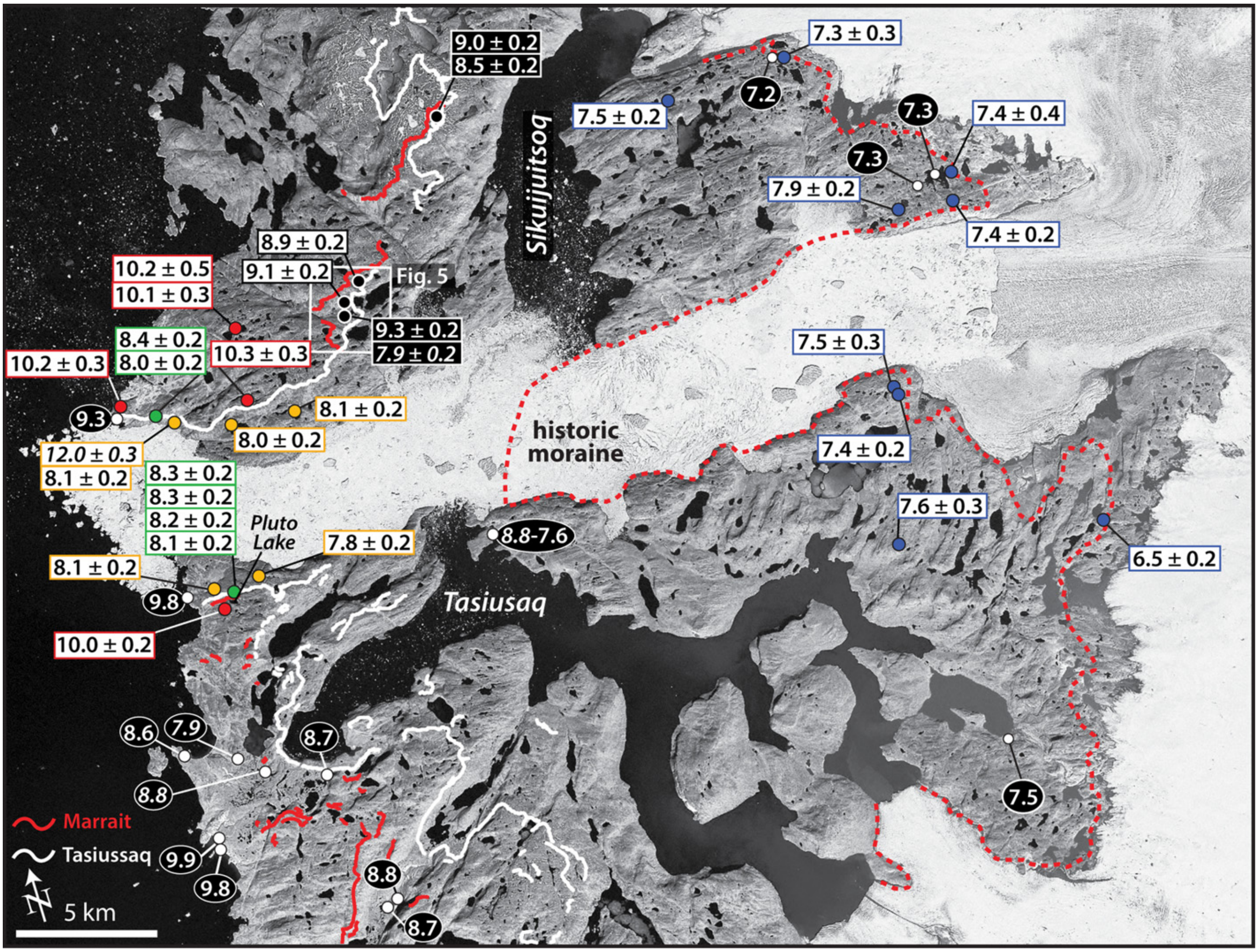

Fig. 2. ^{10}Be and ^{14}C ages relating to early and middle Holocene ice-margin deposits at Jakobshavn Isfjord. ^{10}Be ages (Table 1) are presented in ka at 1σ AMS uncertainty and in 5 distinct morphostratigraphic groups: 1) outboard of the Marrait moraine (red boxes), 2) between the Marrait and Tasiussaq moraines (black), 3) Tasiussaq moraine boulders (green), 4) directly inboard of the Tasiussaq moraine (orange), and 5) near the historic moraine (blue) shown as a dashed red line. ^{10}Be ages from between the Marrait and Tasiussaq moraines in white text are from Corbett et al. (2011). ^{14}C ages (cal yr BP) are shown in white text/black ovals without uncertainty; these are discussed in the text and listed in Table 2 along with their uncertainties and stratigraphic context. ^{10}Be and ^{14}C ages that are considered outliers are in italics (see main text for Discussion). (For interpretation of the references to color in this figure legend, the reader is referred to the web version of this article.)

To explain the origin of the Fjord Stade moraines two distinct concepts have emerged (Kelly, 1985). Because of their widespread distribution, it is hypothesized that moraine deposition was the result of a climatically driven re-advance or stillstand of the western GrIS margin, perhaps related to the 8.2 ka cooling event (Ten Brink and Weidick, 1974; Long and Roberts, 2002). Others, however, favor ice-sheet dynamics related to topographical control on ice-sheet behavior as the primary mechanism for moraine deposition (Weidick, 1985; Warren and Hulton, 1990; Long et al., 2006). For example, ice-sheet dynamics linked to topographical control on ice-sheet behavior accounts for the Fjord Stade moraines' spatial distribution as a result of ice-lobe stability in topographically restricted regions. In the Disko Bugt region (Fig. 1), the Fjord Stade moraine system delimits the ice sheet's position shortly after it exited a marine environment and became primarily terrestrial-based. A marine-to-terrestrial change in ice-margin environment and associated reduction in the rate of ice loss is cited as a potential mechanism for deposition of the Fjord Stade moraines. Under these circumstances, iceberg calving was restricted to only a few marine-terminating glaciers in fjords, and surface ablation at terrestrial-terminating glaciers would have acted as the primary ice-loss process, promoting a more stable ice margin (Weidick, 1985).

3. Methods

We mapped the Fjord Stade moraines across a ~100 km swath of eastern Disko Bugt. At Jakobshavn Isfjord, we collected 28 samples for ^{10}Be dating from ice-sculpted bedrock surfaces, boulders perched on bedrock and Tasiussaq moraine boulders (Fig. 2; Table 1). We sampled five boulders from the Marrait moraine north of Jakobshavn Isfjord, but these samples are still being processed and will ultimately be used for a ^{10}Be production rate calibration experiment. All but two of the samples from the Jakobshavn Isfjord region were previously reported (Young et al., 2011a, 2011b), but to compare these ages with new ^{10}Be ages from Disko Bugt we review all ^{10}Be ages from Jakobshavn Isfjord including sample localities and site-specific interpretations. In southeastern Disko Bugt, we collected 19 samples for ^{10}Be dating from ice-sculpted bedrock surfaces and boulders perched on bedrock, all of which are presented here for the first time.

Table 1
^{10}Be sample information for Jakobshavn Isfjord and SE Disko Bugt.

Sample	Latitude (DD)	Longitude (DD)	Elevation (m asl)[a]	Boulder height (m)	Thickness (cm)	Shielding correction	Quartz (g)	^{9}Be (μg)[b]	$^{10}Be/^{9}Be$ ratio[c]	Uncertainty	^{10}Be (atoms g^{-1})	^{10}Be uncertainty (atoms g^{-1})	^{10}Be age (ka)[d]	Reference
Outboard of Fjord Stade moraines														
Jakobshavn Isfjord														
JAKN08-01	69.2055	−51.1244	96	Bedrock	2.5	1.000	80.05	181	3.19E-13	7.85E-15	4.76E+04	1.17E+03	10.2 ± 0.3 (0.6)	Young et al., 2011a; 2011b
JAKN08-08	69.1993	−50.9674	322	Bedrock	1.0	1.000	85.06	120	6.50E-13	1.83E-14	6.14E+04	1.73E+03	10.3 ± 0.3 (0.6)	Young et al., 2011a; 2011b
JAKN08-21	69.2432	−50.9807	374	Bedrock	1.0	1.000	75.49	154	4.68E-13	2.48E-14	6.39E+04	3.38E+03	10.2 ± 0.5 (0.7)	Young et al., 2011a; 2011b
JAKN08-22	69.2410	−50.9614	344	3.0	4.5	1.000	80.16	159	4.49E-13	1.41E-14	5.96E+04	1.87E+03	10.1 ± 0.3 (0.6)	Young et al., 2011a; 2011b
09GRO-01	69.1098	−51.0414	188	Bedrock	5.0	1.000	77.09	102	5.69E-13	1.42E-14	5.02E+04	1.25E+03	10.0 ± 0.2 (0.5)	Young et al., 2011a; 2011b
Southeastern Disko Bugt														
10GRO-08	68.6695	−50.9987	119	Bedrock	3.5	1.000	58.06	162	2.39E-13	4.57E-15	4.46E+04	8.53E+02	9.4 ± 0.2 (0.5)	This study
10GRO-18	68.6164	−51.0512	164	Bedrock	4.5	1.000	58.78	162	2.51E-13	6.21E-15	4.62E+04	1.14E+03	9.4 ± 0.2 (0.5)	This study
10GRO-33	68.7027	−50.8445	312	Bedrock	3.0	0.998	50.04	162	2.50E-13	4.69E-15	5.40E+04	1.01E+03	9.3 ± 0.2 (0.5)	This study
10GRO-34	68.7000	−50.8209	332	Bedrock	2.0	1.000	53.46	162	2.79E-13	5.24E-15	5.67E+04	1.06E+03	9.5 ± 0.2 (0.5)	This study
Between moraines														
Jakobshavn Isfjord														
09GRO-24	69.2476	−50.7697	300	Bedrock	2.0	1.000	84.04	104	6.19E-13	1.17E-14	5.15E+04	9.69E+02	8.9 ± 0.2 (0.5)	Young et al., 2011b
09GRO-27	69.2372	−50.8373	280	Bedrock	5.0	1.000	50.00	163	2.31E-13	4.46E-15	5.03E+04	9.70E+02	9.1 ± 0.2 (0.5)	Young et al., 2011b
Southeastern Disko Bugt														
10GRO-01	68.6356	−50.9715	105	Bedrock	3.5	1.000	50.14	162	1.97E-13	3.97E-15	4.26E+04	8.60E+02	9.1 ± 0.2 (0.5)	This study
10GRO-10	68.6216	−50.9427	145	Bedrock	4.0	0.997	60.07	162	2.30E-13	5.69E-15	4.15E+04	1.03E+03	8.6 ± 0.2 (0.5)	This study
10GRO-11	68.6216	−50.9423	145	1.0	3.0	0.997	50.11	162	1.89E-13	6.32E-15	4.09E+04	1.37E+03	8.4 ± 0.3 (0.5)	This study
10GRO-25	68.6142	−51.0298	166	Bedrock	2.0	1.000	50.00	163	2.08E-13	4.03E-15	4.53E+04	8.78E+02	9.0 ± 0.2 (0.5)	This study
10GRO-31	68.7090	−50.8077	132	Bedrock	1.0	0.987	50.19	161	2.01E-13	3.79E-15	4.31E+04	8.14E+02	8.9 ± 0.2 (0.5)	This study
10GRO-32	68.7135	−50.8439	85	Bedrock	2.0	0.989	60.20	162	2.30E-13	5.54E-15	4.15E+04	9.97E+02	9.1 ± 0.2 (0.5)	This study
Tasiussaq moraine														
Jakobshavn Isfjord														
FST08-01	69.2022	−51.0878	75	2.50	1.0	0.999	69.93	122	3.34E-13	5.71E-15	3.89E+04	6.62E+02	8.4 ± 0.2 (0.5)	Young et al., 2011b
FST08-02	69.2019	−51.0860	75	2.50	1.0	0.999	82.04	122	3.71E-13	7.30E-15	3.69E+04	7.38E+02	8.0 ± 0.2 (0.4)	Young et al., 2011b
09GRO-08	69.1131	−51.0371	170	1.75	1.0	1.000	64.39	104	3.88E-13	9.62E-15	4.21E+04	1.04E+03	8.3 ± 0.2 (0.4)	Young et al., 2011b
09GRO-09	69.1130	−51.0360	170	1.25	1.0	1.000	87.48	105	5.28E-13	9.99E-15	4.23E+04	8.00E+02	8.3 ± 0.2 (0.4)	Young et al., 2011b
09GRO-11	69.1129	−51.0344	170	1.75	4.0	1.000	85.05	105	4.92E-13	1.14E-14	4.05E+04	9.37E+02	8.1 ± 0.2 (0.4)	Young et al., 2011b
09GRO-12	69.1130	−51.0343	170	1.75	3.0	1.000	86.60	104	5.18E-13	1.20E-14	4.17E+04	9.63E+02	8.2 ± 0.2 (0.4)	Young et al., 2011b
Inboard of Fjord Stade moraines														
Jakobshavn Isfjord														
JAKN08-13	69.1844	−50.9060	175	Bedrock	2.5	1.000	80.17	185	2.66E-13	6.75E-15	4.11E+04	1.04E+03	8.1 ± 0.2 (0.4)	Young et al., 2011a; 2011b
FST08-BR	69.1974	−51.0541	60	Bedrock	2.0	0.999	80.03	102	6.32E-13	1.57E-14	5.38E+04	1.34E+03	12.0 ± 0.3 (0.6)	Young et al., 2011a; 2011b

(*continued on next page*)

Table 1 (*continued*)

Sample	Latitude (DD)	Longitude (DD)	Elevation (m asl)[a]	Boulder height (m)	Thickness (cm)	Shielding correction	Quartz (g)	^{9}Be (μg)[b]	^{10}Be/^{9}Be ratio[c]	Uncertainty	^{10}Be (atoms g^{-1})	^{10}Be uncertainty (atoms g^{-1})	^{10}Be age (ka)[d]	Reference
FST08-04	69.1974	−51.0538	60	2.5	2.0	0.999	80.32	102	4.28E-13	1.11E-14	3.63E+04	9.41E+02	8.1 ± 0.2 (0.4)	Young et al., 2011a; 2011b
09GRO-03	69.1137	−51.0643	119	Bedrock	3.0	1.000	76.80	102	4.39E-13	1.29E-14	3.89E+04	1.14E+03	8.1 ± 0.2 (0.5)	Young et al., 2011a; 2011b
09GRO-06	69.1161	−50.9911	240	2.5	4.5	1.000	74.57	102	4.54E-13	1.45E-14	4.15E+04	1.32E+03	7.8 ± 0.2 (0.4)	Young et al., 2011a; 2011b
09GRO-33	69.1912	−50.9918	120	2.5	4.5	1.000	76.03	102	4.18E-13	1.30E-14	3.75E+04	1.17E+03	8.0 ± 0.2 (0.5)	Young et al., 2011a; 2011b
Southeastern Disko Bugt														
10GRO-07	68.6587	−50.9798	60	Bedrock	1.5	1.000	61.09	162	2.11E-13	4.24E-15	3.75E+04	7.52E+02	8.3 ± 0.2 (0.4)	This study
10GRO-12	68.6219	−50.9385	140	Bedrock	1.5	1.000	60.50	162	2.23E-13	4.45E-15	4.00E+04	7.97E+02	8.1 ± 0.2 (0.4)	This study
10GRO-13	68.6149	−50.9096	144	1.5	2.5	0.994	59.99	162	2.13E-13	6.91E-15	3.86E+04	1.25E+03	7.9 ± 0.2 (0.5)	This study
10GRO-14	68.6153	−50.9027	132	Bedrock	2	0.997	60.03	162	2.21E-13	4.86E-15	4.00E+04	8.77E+02	8.2 ± 0.2 (0.4)	This study
10GRO-28	68.7253	−50.6822	246	Bedrock	3	0.999	60.16	163	2.25E-13	4.45E-15	4.06E+04	8.04E+02	7.5 ± 0.2 (0.4)	This study
10GRO-35	68.7188	−50.5620	198	Bedrock	2.5	0.995	50.14	162	1.63E-13	4.60E-15	3.51E+04	9.95E+02	6.8 ± 0.2 (0.4)	This study
10GRO-39	68.7104	−50.4712	206	Bedrock	1.5	1.000	50.53	162	1.79E-13	3.74E-15	3.85E+04	8.02E+02	7.3 ± 0.2 (0.4)	This study
Historical margin														
Jakobshavn Isfjord														
JAKN08-28	69.2407	−49.9852	215	Bedrock	1.0	1.000	85.09	122	4.12E-13	1.98E-14	3.96E+04	1.90E+03	7.4 ± 0.4 (0.5)	Young et al., 2011a
JAKN08-39	69.2214	−49.9952	206	Bedrock	3.0	1.000	85.37	121	4.08E-13	1.33E-14	3.87E+04	1.26E+03	7.4 ± 0.2 (0.4)	Young et al., 2011a
JAKN08-40	69.2256	−50.0569	147	Bedrock	2.0	1.000	80.03	185	2.52E-13	6.45E-15	3.89E+04	9.97E+02	7.9 ± 0.2 (0.4)	Young et al., 2011a
JAKN08-44	69.3078	−50.1479	347	Bedrock	2.0	1.000	80.22	166	3.21E-13	1.21E-14	4.45E+04	1.68E+03	7.3 ± 0.3 (0.4)	Young et al., 2011a
JAKN08-56	69.3005	−50.3287	425	Bedrock	1.0	1.000	80.01	184	3.21E-13	7.90E-15	4.94E+04	1.21E+03	7.5 ± 0.2 (0.4)	Young et al., 2011a
JAKS08-08	69.0627	−49.8804	371	Bedrock	2.0	1.000	80.04	182	2.65E-13	6.72E-15	4.03E+04	1.02E+03	6.5 ± 0.2 (0.4)	This study
JAKS08-24	69.0694	−50.1478	314	Bedrock	3.0	1.000	80.44	166	3.22E-13	1.44E-14	4.43E+04	1.98E+03	7.6 ± 0.3 (0.5)	This study
JAKS08-33	69.1471	−50.1245	222	Bedrock	1.0	1.000	80.29	165	2.97E-13	1.26E-14	4.07E+04	1.73E+03	7.5 ± 0.3 (0.5)	Young et al., 2011a
JAKS08-34	69.1465	−50.1037	180	Bedrock	2.0	1.000	80.10	184	2.48E-13	6.35E-15	3.80E+04	9.75E+02	7.4 ± 0.2 (0.4)	Young et al., 2011a
Southeastern Disko Bugt														
10GRO-40	68.7026	−50.4267	230	3.5	1.0	1.000	50.16	162	1.75E-13	4.25E-15	3.79E+04	9.20E+02	6.9 ± 0.2 (0.4)	This study
10GRO-41	68.7030	−50.4288	230	Bedrock	1.5	1.000	50.47	162	1.77E-13	4.17E-15	3.80E+04	8.97E+02	7.0 ± 0.2 (0.4)	This study

[a] Uplift-corrected elevation; elevations have been rounded to the nearest meter.
[b] All samples were spiked with a 405 μg/g ^{9}Be carrier.
[c] AMS results are standardized to 07KNSTD3110 (Nishiizumi et al., 2007); ratios are blank-corrected (<1–4% of sample total) and shown at 1-sigma uncertainty.
[d] Be ages given at 1-sigma AMS uncertainties. The external uncertainty is given in parentheses.

3.1. Moraine mapping

We mapped the Fjord Stade moraine complex using 1:40,000 and 1:150,000 scale air photographs acquired in 1953 and 1985, respectively. Our mapping is generally consistent with the original mapping of Weidick (1968, 1974) and later summarized by Weidick and Bennike (2007), but an exact comparison is challenging because published mapping is simplified in some areas. Our mapping focuses on differentiating between Marrait and Tasiussaq moraine crests; our confidence in this distinction varies across Disko Bugt. At Jakobshavn Isfjord and on the Nuuk peninsula (Figs. 2 and 3), all moraines were field checked by walking their crests with a handheld GPS receiver continuously logging positions. Thus, in these areas confidence in mapping is high, particularly when supported by ^{10}Be- or ^{14}C-dating. In the region between Jakobshavn Isfjord and our field area in southeastern Disko Bugt, mapping relies exclusively on air-photo interpretation; however, mapping in this region is consistent with previously mapped moraine crests (e.g. Weidick, 1968; Weidick, 1974).

The Marrait and Tasiussaq moraines divide the Disko Bugt landscape into three distinct morphostratigraphic surfaces: 1) outboard of the Fjord Stade moraines, 2) between the Marrait and Tasiussaq moraines, and 3) inboard of the Tasiussaq moraine. ^{10}Be ages from surfaces located outboard of the Fjord Stade moraines constrain the timing of Disko Bugt deglaciation and also act as maximum limits on the age of the Marrait moraine. ^{10}Be ages from between the Marrait and Tasiussaq moraines are minimum-constraining ages on the Marrait moraine and are maximum-constraining ages on the Tasiussaq moraine. ^{10}Be ages from inboard of the Tasiussaq moraine are minimum-constraining ages for both moraines.

3.2. Field methods: ^{10}Be sample collection

Using a hammer and chisel, we sampled the top several centimeters of bedrock surfaces and boulders (Table 1; Fig. 4). We sampled flat surfaces, and in the case of moraine boulders and perched erratics, we avoided sampling near boulder edges. A clinometer was used to measure shielding by the surrounding topography and a handled GPS receiver with a vertical uncertainty of ~5 m was used to record sample location and elevation. Sample elevations range from ~60 to 425 m asl and all samples were collected from above the local marine limit, which is at least 80 m asl out near the coast, and ~40 m asl inboard the Fjord Stade moraines (Long et al., 2006).

3.3. Quartz and beryllium isolation

Quartz was isolated from whole-rock samples following the procedures of Kohl and Nishiizumi (1992). Samples were first crushed, ground and sieved to isolate the 250–850 μm grain fraction. Next, samples were etched in ultrasonic baths in HCl and dilute HF–HNO_3 mixtures. If needed, samples were passed through heavy liquid to remove acid-resistant mafic minerals. Quartz purity was measured by inductively coupled plasma analysis, and samples were subjected to additional HF–HNO_3 baths until targeted Al purity levels were achieved, generally <75 ppm. All samples were prepared at the University at Buffalo Cosmogenic Nuclide Laboratory.

Quartz dissolution and beryllium isolation procedures followed a slightly modified version of the University of Vermont Cosmogenic Laboratory's beryllium extraction procedures (http://www.uvm.edu/cosmolab/?Page=methods.html). Samples were prepared in five batches of 8 or 12 that each included one process blank and all samples were spiked with ~0.25–0.45 g of a ~405 ppm ^{9}Be carrier (~100–180 μg of ^{9}Be; Table 1). Between ~50 and 85 g of pure quartz was dissolved in hot 48–50% HF and after complete quartz dissolution and drydown, samples were fumed with four additions of $HClO_4$ to drive off fluorides and converted to chloride form with two HCl additions. Samples were passed through anion exchange columns to remove Fe and then converted to sulfate form with two additions of H_2SO_4. Next, samples were passed through cation exchange columns to remove B and separate Ti, Be and Al. The Be fraction was precipitated at ~pH 8 as a hydroxide gel to remove alkalis, dried and then oxidized to produce BeO. BeO was mixed with Nb powder and packed into stainless steel targets for accelerator mass spectrometry (AMS) measurements.

3.4. AMS measurements

All ^{10}Be/^{9}Be ratios were measured at the Center for Mass Spectrometry, Lawrence Livermore National Laboratory and normalized to standard 07KNSTD3110 with a reported ratio of 2.85×10^{-12} (Nishiizumi et al., 2007; Rood et al., 2010). Measured sample ratios ranged between 1.62×10^{-13} and 6.49×10^{-13}. Procedural blank ratios were 4.9×10^{-15}, 1.2×10^{-14}, 5.2×10^{-15}, 2.2×10^{-15} and 1.52×10^{-15} equating to ~33,300, 93,940, 37,000, 23,330 and 16,470 ^{10}Be atoms, respectively. Sample ratios were corrected using batch-specific blank values, which were <1–4% of the sample total. One-sigma analytical uncertainties on blank-corrected samples range from 1.7 to 5.3% and average 2.6% (Table 1).

3.5. ^{10}Be age calculations

^{10}Be ages were calculated using the CRONUS-Earth online exposure age calculator (Balco et al., 2008; version 2.2 constants 2.2). Following previous work in the Disko Bugt region (Corbett et al., 2011; Young et al., 2011a, 2011b), we used the northeast North American (NENA) ^{10}Be production rate of 3.91 ± 0.19 atoms g^{-1} yr^{-1} and the Lal/Stone constant-production scaling scheme to calculate ^{10}Be ages (Lal, 1991; Stone, 2000; Balco et al., 2009). We use the NENA ^{10}Be production rate (vs. the globally calibrated ^{10}Be production rate) because calculated ^{10}Be ages are only consistent with the independent radiocarbon control from the region when using the NENA ^{10}Be production rate. By comparison, using the global ^{10}Be production rate would result in exposure ages that are ~12% younger than NENA-derived ^{10}Be ages. We use the Lal/Stone constant-production scaling scheme because the influence of the Earth's magnetic field on ^{10}Be production rate is negligible at the study area's high latitude (~69° N; Gosse and Phillips, 2001); however use of alternative scaling schemes results in ^{10}Be ages that vary by up to ~4%. A full discussion regarding the choice of ^{10}Be production rate and independent radiocarbon control can be found in Briner et al. (2012). The CRONUS-Earth calculator makes sample-specific corrections for latitude, elevation, sample thickness and sample density (2.65 g cm^{-3}; Table 1). Reported age uncertainties for individual samples in Section 4 reflect 1σ AMS uncertainty only ("internal" uncertainty reported from the CRONUS-Earth website), and does not include potential error associated with the addition of ^{9}Be carrier or correction of sample elevation (see below). Using internal AMS uncertainties allows us to investigate relationships between ^{10}Be ages across both field sites. To compare ^{10}Be ages to independent ^{14}C ages in Sections 5, however, we include the external uncertainty when reporting ^{10}Be ages by propagating the 1σ production rate uncertainty in the quadrature.

We made no corrections for surface erosion or shielding by snow cover. The crystalline bedrock in the region is resistant to erosion, and glacial striations were routinely observed on sample surfaces indicating little, if any surface erosion has occurred since deglaciation. Thus, we consider the effects of erosion on calculated

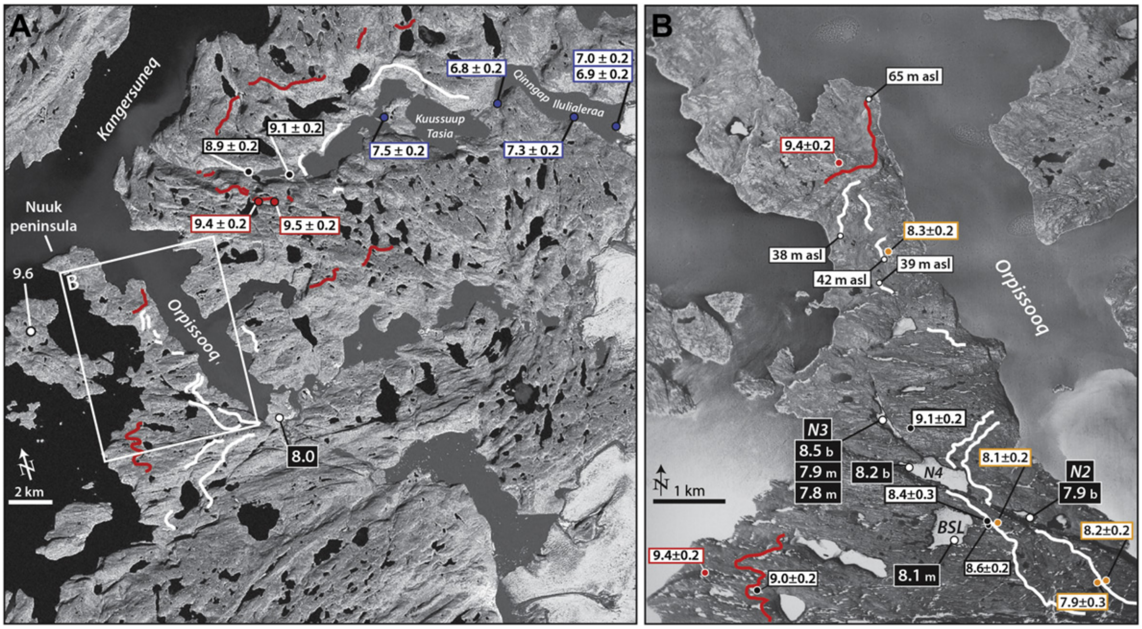

Fig. 3. Southeastern Disko Bugt. (A) Nuuk peninsula and Kuussuup Tasia region showing Marrait and Tasiussaq moraine crests and ^{10}Be (ka; 1σ) and ^{14}C ages. (B) The Marrait and Tasiussaq moraines on Nuuk peninsula with ^{10}Be ages and elevations of where moraine crests disappear below marine limit. BSL – Big Square Lake. "b" – ^{14}C age from bulk sediments (Long and Roberts, 2002). "m" – ^{14}C age from macrofossils (this study). Colorway is the same as in Fig. 2. (For interpretation of the references to color in this figure legend, the reader is referred to the web version of this article.)

^{10}Be ages to be negligible, particularly on the Holocene timescales considered here. All of our samples, including bedrock samples, were collected from locally high windswept locations and we observe no correlation between boulder height and ^{10}Be age on moraine boulders, which might be expected with significant snow cover. Using meteorological data from the Jakobshavn Isfjord region, however, Corbett et al. (2011) estimated that reported ^{10}Be ages without a correction for snow cover could underestimate true ages by no more than ~7%. This is likely a significant overestimate because this correction does not account for sample location (e.g.

Fig. 4. (A) Boulder perched on bedrock located outboard of the Marrait moraine at Jakobshavn Isfjord. (B) Boulder perched on bedrock located immediately outboard of the Tasiussaq moraine system on the Nuuk peninsula. (C) Sampled boulder near the current ice margin in southeastern Disko Bugt. In this picture, the historic moraine (dashed line) abuts a boulder that was deposited 6.9 ± 0.2 ka. (D) On the Nuuk peninsula, the Marrait moraine grades to a delta at 65 m asl. Donner and Junger (1975) also described this delta surface and obtained an elevation of 62 m asl.

windswept locations), and assumes all snow remains on the landscape during the winter months.

The Disko Bugt region has undergone glaciostatic uplift since deglaciation, and the sample elevation at the time of collection does not reflect its time-averaged sample elevation history. Following Young et al. (2011a, 2011b), we use published relative sea-level data from the region to calculate sample-specific elevation corrections (Long and Roberts, 2002; Long et al., 2006). Samples outboard of the Fjord Stade moraines require an elevation correction of −15.6 m, −5.0 m for samples located between Fjord Stade moraines and −4.6 m for all remaining samples. For samples located outboard of the Fjord Stade moraines, this elevation correction equates to ^{10}Be ages that are ~2% older than ^{10}Be ages calculated without a corrected elevation. ^{10}Be ages calculated for all remaining samples using uplift-corrected elevations are <1% older than ^{10}Be ages calculated without an elevation correction. In general, uplift corrections are within the 1σ AMS sample uncertainties (1.7–5.3%) and although we present ^{10}Be ages corrected for glacioisostatic uplift, this correction does not significantly change our ^{10}Be ages or our interpretations.

4. Results

4.1. The Fjord Stade moraines in Disko Bugt

At Jakobshavn Isfjord, the Fjord Stade moraines are generally well defined and single-crested (Fig. 2). Immediately south of the fjordmouth, the Marrait and Tasiussaq moraines are closely nested and the Marrait and Tasiussaq moraines grade to raised shorelines resting at ~65 and ~40 m asl, respectively. On the northern side of the fjordmouth, only the Tasiussaq moraine is present, and while walking the Tasiussaq moraine crest, we identified three locations where the moraine disappears at elevations below ~45–40 m asl, before reappearing again at higher elevations. To the north and slightly up-fjord, the Marrait moraine emerges from beneath the Tasiussaq moraine (Figs. 2 and 5).

At the southeastern Disko Bugt location on the Nuuk peninsula, the landscape is dominated by the Tasiussaq moraine system, which is composed of two adjacent moraine ridges, whereas only a few segments of the Marrait system are preserved (Fig. 3). Similar to the Jakobshavn Isfjord region, we identified locations where the Marrait moraine grades to a ~65 m asl raised delta surface and the Tasiussaq moraine disappear below ~40 m asl (Figs. 3 and 4). Moraine crests on the Nuuk peninsula are interpreted to be left-lateral moraines deposited by an ice lobe that originated from the southeast.

Northeast of the Nuuk peninsula, both moraine systems are present, but we only field checked moraine segments adjacent to our ^{10}Be sample locations (Fig. 3). The most prominent moraine (Tasiussaq) in this region dams the Kuussuup Tasia valley, and similar to the landscape between the Marrait and Tasiussaq moraines at Jakobshavn Isfjord, the landscape surrounding Kuussuup Tasia is mainly till covered.

4.2. ^{10}Be ages from Jakobshavn Isfjord

^{10}Be ages at Jakobshavn Isfjord range from 12.0 ± 0.3 to 6.5 ± 0.2 ka (Table 1). ^{10}Be ages from bedrock surfaces ($n = 4$) and a perched boulder ($n = 1$) outboard of the Fjord Stade moraines have a mean of 10.2 ± 0.1 ka (1σ) and two bedrock samples from between the Marrait and Tasiussaq moraines have ^{10}Be ages of 9.1 ± 0.2 and 8.9 ± 0.2 ka (Table 1; Figs. 2 and 6). Six boulders from the Tasiussaq moraine range between 8.4 ± 0.2 and 8.0 ± 0.2 ka (mean = 8.2 ± 0.2 ka) and five ^{10}Be ages from bedrock surfaces ($n = 2$) and perched boulders ($n = 3$) just inboard of the Tasiussaq moraine have a mean ^{10}Be age of 8.0 ± 0.2 ka after excluding one older outlier from a bedrock surface (FST08-BR; 12.0 ± 0.3 ka) that is >3σ older than remaining ^{10}Be ages. Nine samples from polished bedrock near the historic margin yield ^{10}Be ages that range from 7.9 ± 0.2 to 6.5 ± 0.2 ka (Table 1).

4.3. ^{10}Be ages from Southeastern Disko Bugt

On the Nuuk peninsula, two ^{10}Be ages from bedrock surfaces immediately outboard of the Marrait moraine are each 9.4 ± 0.2 ka and four ^{10}Be ages (3 bedrock; 1 boulder) from between the Marrait and Tasiussaq moraines range from 9.1 ± 0.2 to 8.4 ± 0.2 ka (Fig. 3). ^{10}Be ages from bedrock ($n = 3$) and one boulder inboard of the Tasiussaq moraine are between 8.3 ± 0.2 and 7.9 ± 0.3 ka. In both areas, boulder ages are statistically the same as bedrock ages.

Northeast of the Nuuk peninsula, two bedrock ^{10}Be ages outboard of the Marrait moraine are 9.5 ± 0.2 and 9.4 ± 0.2 ka (Fig. 3). Two ^{10}Be ages from bedrock between the Marrait and Tasiussaq moraines are 9.1 ± 0.2 and 8.9 ± 0.2 ka. Five ^{10}Be ages (4

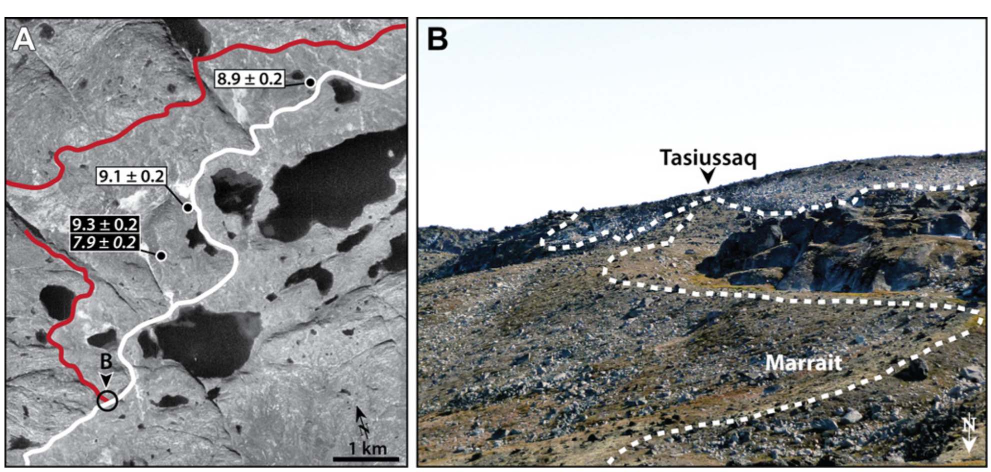

Fig. 5. (A) Region north of Jakobshavn Isfjord where the Marrait and Tasiussaq moraines are separated (map location shown in Fig. 2). ^{10}Be ages from this landscape are close minimum-constraining ages on deposition of the Marrait moraine (ages in white text are from Corbett et al., 2011). Arrow points to the location where the Tasiussaq moraine truncates the Marrait moraine indicating that Jakobshavn Isbræ advanced to deposit the Tasiussaq moraine. (B) Juncture between the Marrait and Tasiussaq moraines. White dashes follow the crest of Marrait moraine and the base of the Tasiussaq moraine.

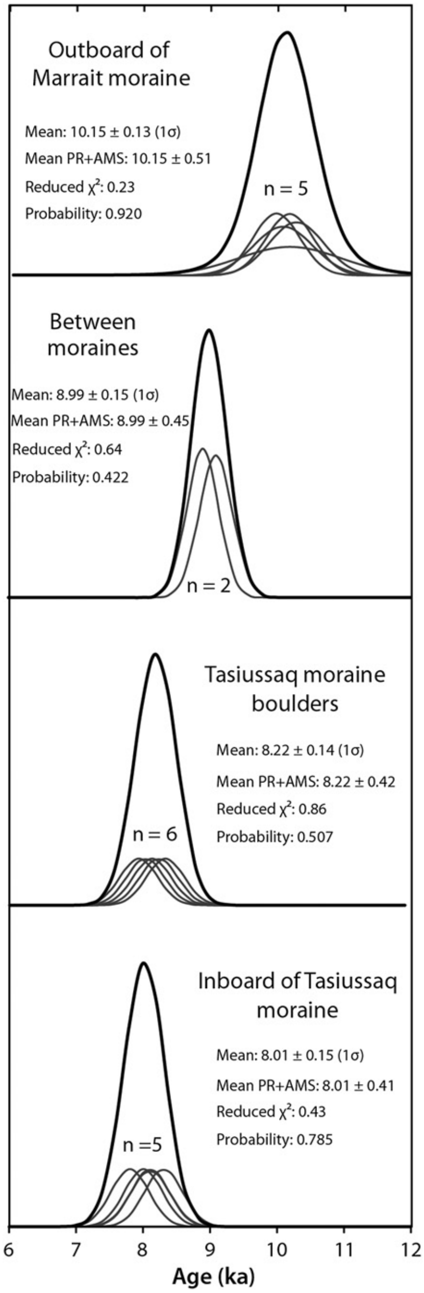

Fig. 6. Normal kernel density estimates of ^{10}Be ages (1σ) from key morphostratigraphic surfaces at Jakobshavn Isfjord. The *y*-axis is relative probability in all plots. Mean PR + AMS − mean age with NENA (external) production rate uncertainty (~4.8%) and AMS uncertainty propagated in the quadrature.

bedrock; 1 boulder) along a transect extending through the Kuussuup Tasia valley from inboard of the Tasiussaq moraine to the current ice margin range from 7.5 ± 0.2 to 6.9 ± 0.2 ka.

5. The age of the Fjord Stade moraine complex

5.1. Jakobshavn Isfjord

At Jakobshavn Isfjord, ^{10}Be ages indicate that the GrIS retreated out of Disko Bugt and made landfall ~10.2 ± 0.5 ka [n = 5; error term has production rate (PR) uncertainty propagated through]. The timing of deglaciation is consistent with: 1) a basal ^{14}C age of 10,370 ± 130 cal yr BP (2σ) from a marine-sediment core in the middle of Disko Bugt (Fig. 1; Lloyd et al., 2005), 2) an average ^{10}Be age of 10.5 ± 0.6 ka (n = 7; PR uncertainty included) from the same landscape reported in Corbett et al. (2011), and 3) minimum-constraining ^{14}C ages from raised marine sediments near the Jakobshavn fjordmouth, the oldest of which is ~9.9 cal ka BP (Figs. 1 and 2; Table 1; Weidick and Bennike, 2007).

A series of ^{14}C and ^{10}Be ages limit the age of the Marrait and Tasiussaq moraines. On the southern side of Jakobshavn Isfjord, ^{14}C-dated marine sediments located inland of the Marrait moraine and buried by Tasiussaq outwash provide minimum- and maximum-constrains on deposition of the Marrait and Tasiussaq moraines, respectively. These ages are 8800 ± 340, 8750 ± 220, 8670 ± 260, 8570 ± 400 and 7930 ± 270 cal yr BP (Fig. 2; Table 2; Weidick and Bennike, 2007). The most unambiguous age control on the Marrait moraine comes from Pluto Lake, a proglacial-threshold lake (e.g. Briner et al., 2010) directly adjacent to the moraine (Fig. 2). ^{14}C ages from the lower and upper contacts of a ~1.5-m-thick minerogenic sediment layer that was deposited in the lake during emplacement of the Marrait moraine provide maximum- and minimum-constraining ages on the Marrait moraine. Bracketing ^{14}C ages of 9190 ± 100 and 9140 ± 110 cal yr BP from the lower contact and 9210 ± 80 and 9150 ± 120 cal yr BP from the upper contact constrain Marrait moraine deposition to ~9.2 ka, consistent with the aforementioned minimum ^{14}C ages. In addition, the lake's sediment stratigraphy, alternating units of organic- and minerogenic-rich sediments, indicates that the Marrait moraine was deposited following a re-advance of Jakobshavn Isbræ (Young et al., 2011b).

Further supporting the ~9.2 ka age of the Marrait moraine are ^{10}Be ages inboard of the Marrait moraine north of Jakobshavn Isfjord (Figs. 2 and 5). ^{10}Be ages of 9.1 ± 0.5 and 8.9 ± 0.5 ka (error terms includes PR uncertainty) are minimum ages for deposition of the Marrait moraine, consistent with the Pluto Lake's ^{14}C chronology. Moreover, Corbett et al. (2011) obtained ^{10}Be ages of 9.3 ± 0.5 and 7.9 ± 0.4 ka from this same region. The younger ^{10}Be age is from a bedrock surface and is likely too young, perhaps influenced by post-deglaciation sediment shielding; however, the older age is compatible with remaining ^{10}Be ages from this region (Fig. 5). Corbett et al. (2011) also presented two ^{10}Be ages of 9.0 ± 0.5 and 8.5 ± 0.5 ka from a separate location between the Marrait and Tasiussaq moraines farther north of the Isfjord (Fig. 2); again these are minimum-constraining ages on deposition of the Marrait moraine. Taken together, ^{10}Be ages from inboard of the Marrait moraine support the ~9.2 ka age of the moraine as constrained by ^{14}C ages from south of Jakobshavn Isfjord.

^{10}Be ages from Tasiussaq moraine boulders date a re-advance of Jakobshavn Isbræ culminating 8.2 ± 0.4 ka (n = 6). Evidence for a re-advance comes from a location north of the Isfjord where the Tasiussaq moraine truncates the Marrait moraine (Fig. 5). Supporting the ~8.2 ka age of the Tasiussaq moraine are ^{10}Be ages immediately inboard of the moraine indicating that Jakobshavn Isbræ had retreated off the Tasiussaq moraine position by 8.0 ± 0.4 ka (n = 5; Figs. 2 and 6). These ages are from both ice-sculpted bedrock and erratics perched on bedrock; there is no indication that these ages are influenced by inheritance of ^{10}Be from prior periods of exposure (e.g. Corbett et al., 2011). Furthermore, two ^{10}Be ages reported by Corbett et al. (2011) from directly inboard of the Tasiussaq moraine average 8.2 ± 0.4 ka.

In addition to ^{10}Be ages, a series of ^{14}C ages from the same landscape help limit the depositional timing of the Tasiussaq moraine. Four basal ^{14}C ages from bulk sediments from lake sediment cores located up-fjord of the Tasiussaq moraine are 8820 ± 180, 7740 ± 80, 7600 ± 80 and 7590 ± 80 cal yr BP (Long

Table 2
Radiocarbon ages that constrain the ice-margin position in the Jakobshavn Isfjord region and SE Disko Bugt, western Greenland.

Sample ID	Locality	Latitude (N)	Longitude (W)	^{14}C yr BP	Cal yr BP	Context	Reference
Outboard of both Fjord Stade moraines[M]							
AAR-5	Disko Island	69° 17′	53° 28′	9650 ± 125	10,495 ± 150	Shells in marine silts underlying lake sediments, minimum age on initial deglaciation	Ingólfsson et al., 1990
AA-37711	Central Disko Bugt	69° 11′	51° 49′	9485 ± 65	10,370 ± 130	Marine core POR18, Disko Bugt, minimum age on initial deglaciation	Lloyd et al., 2005, Table 1
AA39655	SE Disko Bugt	68° 37′	52° 06′	9180 ± 80	10,390 ± 170	Lake IV7 basal sediment bulk AMS age	Long et al., 2003
Ua-1086	Jakobshavn Isfjord	69° 12′	51° 04′	8795 ± 130	9470 ± 350	Raised marine deposits	Weidick and Bennike, 2007, Table 3
K-1818	Jakobshavn Isfjord	69° 06′	51° 04′	8630 ± 130	9790 ± 370	Raised marine deposits	Weidick and Bennike, 2007, Table 3
Ua-4574	Jakobshavn Isfjord	69° 00′	50° 58′	9180 ± 75	9950 ± 230	Raised marine deposits	Weidick and Bennike, 2007, Table 3
K-2023	Jakobshavn Isfjord	69° 01′	51° 08′	8680 ± 135	9820 ± 340	Raised marine deposits	Weidick and Bennike, 2007, Table 3
AA-39659	SE Disko Bugt	68° 40′	51° 07′	8585 ± 86	9610 ± 180	Lake AK4 basal sediment bulk AMS age	Long and Roberts, 2002
Maximum age of Marrait moraine deposition							
CURL-11376	Jakobshavn Isfjord	69° 06′	51° 02′	8225 ± 20	9190 ± 100	AMS age on plant macrofossils, Pluto Lake, maximum age on Tasiussaq moraine deposition	Young et al., 2011b
CURL-11061	Jakobshavn Isfjord	69° 06′	51° 02′	8180 ± 25	9140 ± 110	AMS age on plant macrofossils, Pluto Lake, maximum age on Tasiussaq moraine deposition	Young et al., 2011b
Minimum age of Marrait moraine deposition							
CURL-12594	Jakobshavn Isfjord	69° 06′	51° 02′	8245 ± 20	9210 ± 80	AMS age on plant macrofossils, Pluto Lake, minimum age on Tasiussaq moraine deposition	Young et al., 2011b
CURL-11374	Jakobshavn Isfjord	69° 06′	51° 02′	8210 ± 20	9150 ± 120	AMS age on plant macrofossils, Pluto Lake, minimum age on Tasiussaq moraine deposition	Young et al., 2011b
Maximum age of Tasiussaq moraine deposition[M]							
K-992	Jakobshavn Isfjord	69° 02′	51° 01′	7110 ± 140	7930 ± 270	Lersletten plain, marine seds overlain by Tasiussaq outwash	Weidick and Bennike, 2007, Table 3
K-993	Jakobshavn Isfjord	68° 56′	50° 58′	7650 ± 140	8570 ± 400	Marine seds overlain by Tasiussaq outwash	Weidick and Bennike, 2007, Table 3
Ua-4575	Jakobshavn Isfjord	69° 02′	50° 56′	8140 ± 95	8670 ± 260	Marine seds overlain by Tasiussaq outwash	Weidick and Bennike, 2007, Table 3
Ua-4573	Jakobshavn Isfjord	68° 56′	50° 53′	8215 ± 80	8750 ± 220	Marine seds overlain by Tasiussaq outwash	Weidick and Bennike, 2007, Table 3
K-2022	Jakobshavn Isfjord	69° 03′	51° 08′	7690 ± 120	8800 ± 340	Marine seds overlain by Tasiussaq outwash	Weidick and Bennike, 2007, Table 3
Minimum age of Tasiussaq moraine deposition							
K-987*	Jakobshavn Isfjord	69° 02′	51° 01′	7850 ± 190	8790 ± 465	Basal age from lake resting on glaicio-fluvial sands at Tasiussaq; see note below	Weidick and Bennike, 2007, Table 3; Tauber (1968)
Beta-178168	Jakobshavn Isfjord	69° 06′	50° 38′	7960 ± 40	8820 ± 180	Lake T5 basal sediment bulk AMS age	Long et al., 2006, Table 1
Beta-178170	Jakobshavn Isfjord	69° 07′	50° 35′	6910 ± 40	7740 ± 80	Lake T7 basal sediment bulk AMS age	Long et al., 2006, Table 1
Beta-178169	Jakobshavn Isfjord	69° 07′	50° 37′	6750 ± 40	7590 ± 80	Lake T6 basal sediment bulk AMS age	Long et al., 2006, Table 1
Beta-178165	Jakobshavn Isfjord	69° 07′	50° 40′	6760 ± 40	7600 ± 80	Lake T4 basal sediment bulk AMS age	Long et al., 2006, Table 1
KIA-23028	Pâkitsoq	69° 29′	50° 42′	6810 ± 40	7660 ± 40	Lake P3, basal sediment bulk AMS age	Long et al., 2006, Table 1
OS-85087	SE Disko Bugt	68° 37′	50° 57′	7220 ± 40	8060 ± 100	Nuuk peninsula, Big Square lake, basal AMS age on plant macrofossils	This study
CURL-12698	SE Disko Bugt	68° 38′	50° 58′	7030 ± 25	7865 ± 70	Nuuk peninsula, Lake N3, basal AMS age on plant macrofossils	This study
CURL-12693	SE Disko Bugt	68° 38′	50° 58′	6975 ± 25	7825 ± 100	Nuuk peninsula, Lake N3, basal AMS age on plant macrofossils	This study
AA-39665	SE Disko Bugt	68° 38′	50° 58′	7733 ± 56	8505 ± 95	Nuuk peninsula, Lake N3, basal sediment bulk AMS age	Long and Roberts, 2002
AA-39664	SE Disko Bugt	68° 38′	50° 58′	7414 ± 72	8210 ± 165	Nuuk peninsula, Lake N4, basal sediment bulk AMS age	Long and Roberts, 2002
AA-39661	SE Disko Bugt	68° 38′	50° 58′	7059 ± 62	7875 ± 125	Nuuk peninsula, lake N2, basal sediment bulk AMS age	Long and Roberts, 2002
Hel-369	SE Disko Bugt	68° 37′	50° 51′	7210 ± 170	8035 ± 325	Raised marine deposits	Donner and Junger, 1975
Minimum age of deglaciation inland of historical moraine							
CURL-11141	Jakobshavn Isfjord	68° 58′	50° 04′	7040 ± 20	7520 ± 55	Raised marine deposits; Hiatella arctica	Briner et al., 2010, Table 1
CURL-10441	Jakobshavn Isfjord	69° 14′	50° 02′	6360 ± 25	7300 ± 120	Iceboom lake, basal sediment macrofossil AMS age, minimum age	Briner et al., 2010, Table 1

(*continued on next page*)

Table 2 (*continued*)

Sample ID	Locality	Latitude (N)	Longitude (W)	^{14}C yr BP	Cal yr BP	Context	Reference
CURL-10090	Jakobshavn Isfjord	69° 19′	50° 11′	6290 ± 15	7210 ± 40	SOV lake, basal sediment macrofossil AMS age, minimum age	Briner et al., 2010, Table 1
CURL-12603	Jakobshavn Isfjord	69° 14′	50° 02′	6185 ± 15	7090 ± 80	NOR, from 100 cm depth, extrapolated age to basal contact @102 cm is 7295 ka	Young et al., 2011a; Briner et al., 2012

Notes: All radiocarbon ages were calibrated using CALIB html version 6.0 with INTCAL09 (Stuiver et al., 2005). We report calibrated ages at 2-sigma uncertainty rounded to the nearest half decade. K- and Hel-dates are treated as atmospheric samples because they were originally normalized to 0 per mil PDB instead of −25 per mil; M = carbonate material was dated, bivalves were corrected for the standard reservoir value (delta $R = 0$; A. Jennings pers. comm., McNeely et al., 2006; Coulthard et al., 2010). We report sample K-987*, and its morphostratigraphic context, however, this age is older than underlying marine sediments and following Weidick and Bennike (2007) is discounted.

et al., 2006; Fig. 2; Table 2). Because these ^{14}C ages are inboard of the Tasiussaq moraine, they are minimum constraints on the timing of Tasiussaq moraine deposition and the youngest three of these ages are consistent with the 8.2–8.0 ka age of the Tasiussaq moraine as constrained by the ^{10}Be-based chronology. At Pâkitsoq, ~25 km north of Jakobshavn Isfjord (Fig. 1), a basal lake sediment ^{14}C age from bulk sediments of 7660 ± 40 cal yr BP immediately inboard of the Tasiussaq moraine also supports the 8.2–8.0 ka age of the Tasiussaq moraine (Long et al., 2006; Table 2). After considering the ^{10}Be and ^{14}C ages from the Jakobshavn Isfjord region that directly relate to the Tasiussaq moraine, the minimum ^{14}C age of 8820 ± 180 cal yr BP is perhaps an old outlier. In addition, the maximum ^{14}C age of 7930 ± 270 cal yr BP (see above; Table 2) is younger than ^{14}C and ^{10}Be ages from inboard of the Tasiussaq moraine, which is a morphostratigraphically younger surface, and thus this ^{14}C age is likely a young outlier. Finally, the three locations at Jakobshavn Isfjord where the Tasiussaq moraine disappears at elevations below 40–45 m asl reveals that the Tasiussaq moraine was emplaced contemporaneous with a relative sea level 40–45 m asl. Using the well-constrained regional emergence curve of Long et al. (2006), a relative sea level of 40–45 m asl dates to ca 8.0–8.2 ka, thus further supporting the 8.2–8.0 ka age of the Tasiussaq moraine as constrained by ^{10}Be ages.

The glacial history following deposition of the Fjord Stade moraines is constrained by a series of ^{10}Be ages just beyond (typically within ~20 m) the moraine near the present ice margin [herein historical moraine; Weidick, 1968; in many place the historical terminal moraine was deposited during the Little Ice Age (~1300–1900 AD), yet in other places it was deposited during the 20th century; Kelly and Lowell, 2009]. The ^{10}Be ages reveal that Jakobshavn Isbræ had retreated through its fjord at a rate of ~100 m yr^{-1} and likely behind its current margin by 7.5 ± 0.4 ka (Fig. 2; Young et al., 2011a). Furthermore, basal ^{14}C ages from three lakes located adjacent to the current ice margin are 7300 ± 120, 7210 ± 40 and 7090 ± 40 cal yr BP, consistent with the ^{10}Be-based timing of local deglaciation (Briner et al., 2010; Young et al., 2011a, Fig. 2; Table 2). ^{10}Be ages near the present ice-sheet margin in Sikuijuitsoq fjord to the north indicate that this margin had retreated behind its current position by 7.6 ± 0.4 ka ($n = 6$), contemporaneous with Jakobshavn Isbræ's retreat (Corbett et al., 2011). A ^{10}Be age of 7.6 ± 0.6 ka ~5 km south of Jakobshavn Isfjord suggests that this sector of the GrIS retreated in concert with Jakobshavn Isbræ. However, a single ^{10}Be age of 6.5 ± 0.4 ka just outboard of the historical moraine is ~1 ka younger than remaining ^{10}Be ages near the historical moraine and a ^{14}C age of 7520 ± 55 cal yr BP from raised marine deposits to the south (Fig. 2; Table 2). This younger ^{10}Be age could have been influenced by post-deglaciation sediment shielding, or it may record the delayed deglaciation of the GrIS margin directly south of Jakobshavn Isfjord; however, all remaining ^{10}Be and ^{14}C ages from the region suggest that the broader GrIS margin had retreated behind its present position ~7.5 ka (Corbett et al., 2011; Young et al., 2011a).

5.2. Southeastern Disko Bugt

Deglaciation of southern Disko Bugt is constrained by a basal ^{14}C age from lake sediments of 10,390 ± 170 cal yr BP (Long et al., 2003) and ~40 km to the east, a basal ^{14}C age from lake sediments of 9610 ± 180 cal yr BP (Long and Roberts, 2002) marks the timing of deglaciation of inner Disko Bugt (Long et al., 2011; Fig. 1; Table 2). Landscapes immediately outboard of the Marrait moraine at two locations in southeastern Disko Bugt have ^{10}Be ages between ~9.5 and 9.4 ka ($n = 4$; Fig. 3). On both the Nuuk peninsula and at the mouth of the Kuussuup Tasia valley, these ^{10}Be ages are within ~50 m outboard of the Marrait moraine and are thus closely limiting maximum ages on the Marrait moraine. On the Nuuk peninsula, a ^{10}Be age of 9.0 ± 0.5 ka located ~10 m inboard of the Marrait moraine is a minimum age on Marrait moraine deposition (Fig. 3). This age is supported by a ^{10}Be age of 9.1 ± 0.5 ka inboard of the Marrait moraine located ~3 km to the northeast on the Nuuk peninsula. Furthermore, the Marrait moraine here grades a ~65 m asl delta which dates to at least ca 9 ka using regional emergence data (Fig. 4; Long et al., 2006). At the mouth of the Kuussuup Tasia valley, additional ^{10}Be ages of 9.1 ± 0.5 and 8.9 ± 0.5 ka inboard of the Marrait moraine there are minimum-limiting ages. Taken together, the range of ^{10}Be ages from two locations in southeastern Disko Bugt indicate that deposition of the Marrait moraine must have occurred between ~9.4 and 9.0 ka (Fig. 3).

On the Nuuk peninsula, ^{10}Be ages directly outboard of the Tasiussaq moraine system are 8.6 ± 0.5 and 8.4 ± 0.5 ka and ^{10}Be ages within, and inboard of, the Tasiussaq moraine system range from 8.3 ± 0.4 ka to 7.9 ± 0.5 ka. The mean ^{10}Be age from outboard and inboard of the Tasiussaq moraine brackets deposition of the Tasiussaq moraine to ~8.5–8.1 ka (Fig. 3). In addition, the Tasiussaq moraine on the Nuuk peninsula disappears below an elevation of ~40 m asl, further supporting the ^{10}Be-based age of the moraine. This elevation is similar to the elevation at Jakobshavn Isfjord at which the Tasiussaq moraine disappears below, which also dates to ca 8 ka (Long et al., 2006).

Additional chronological constraints on the deposition of the Tasiussaq moraine system are available from ^{14}C ages of basal sediments from several lakes on the Nuuk Peninsula. A basal ^{14}C age of 8060 ± 100 cal yr BP from aquatic macrofossils in Big Square Lake (informal name; Fig. 3) provides a minimum-constraining age on deposition of the Tasiussaq moraine. Big Square Lake rests outboard of the Tasiussaq moraine, but because the Tasiussaq moraine lies within Big Square Lake's catchment, the basal ^{14}C age constrains retreat of the GrIS margin off the Tasiussaq moraine. In contrast to the sediment stratigraphy in Pluto Lake at Jakobshavn Isfjord, Big Square Lake's sediment stratigraphy only consists of minerogenic sediments overlain by organic sediments suggesting that the GrIS margin experienced a stillstand during deposition of the Tasiussaq moraine.

Long and Roberts (2002) obtained basal ^{14}C ages of 8505 ± 95 and 8210 ± 165 cal yr BP from lakes N3 and N4 located adjacent to

Big Square Lake (Fig. 3; Table 2). The Tasiussaq moraine dams lake N4 on its eastern shore and when the GrIS was at the Tasiussaq moraine, N3 and N4 were connected by a small channel. Thus, as with Big Square Lake, N3 and N4 basal ^{14}C ages are minimum ages on deposition of the Tasiussaq moraine. Basal ^{14}C ages from N3 and N4 are slightly older than the ^{14}C age from Big Square Lake (8060 ± 100 cal yr BP); however, the N3 and N4 ^{14}C ages are from bulk sediments, which have been shown to be ~100–400 years too old at some sites on western Greenland when compared to ^{14}C ages from macrofossils at the same stratigraphic level (Kaplan et al., 2002; McGowan et al., 2003; Bennike et al., 2010). We collected new sediment cores from lake N3 and ^{14}C-dated macrofossils in basal sediments in two different cores, which yielded ages of 7865 ± 70 and 7825 ± 100 cal yr BP. A ^{14}C age from marine deposits located inland of the Tasiussaq moraine system at the head of Orpissooq fjord is 8035 ± 325 cal yr BP (Fig. 3; Donner and Junger, 1975) and a basal ^{14}C age from lake N2, which is located inboard of the Tasiussaq moraine system is 7875 ± 125 cal yr BP (Long and Roberts, 2002). These ages provide unambiguous minimum constraints on Tasiussaq moraine deposition. Taken together, ^{10}Be and ^{14}C ages on the Nuuk peninsula indicate that the Tasiussaq moraine system was likely deposited just prior to ~8 ka. Finally, a transect of ^{10}Be ages through the Kuussuup Tasia valley indicates that following deposition of the Tasiussaq moraine, the GrIS retreated through the Kuussuup Tasia valley at ~15 m yr^{-1} and likely retreated behind its current margin at ~7 ka (Fig. 3).

6. Discussion

6.1. Early Holocene abrupt climate change and synchronous deposition of the Fjord Stade moraines

At Jakobshavn Isfjord, the Marrait moraine was deposited ~9.2 ka; in southeastern Disko Bugt, the Marrait moraine was deposited between ~9.4 and 9.0 ka. These data suggest that moraine deposition at localities separated by ~60 km was contemporaneous within dating uncertainties. Our ice-margin chronology also indicates that the Tasiussaq moraine at Jakobshavn Isfjord and in southeastern Disko Bugt was deposited ca 8.2–8.0 ka. Although the exact location and preservation of the Fjord Stade moraines at both locations may be influenced by the interaction between ice dynamics and topography (e.g. Warren and Hulton, 1990; Long et al., 2006), synchronous deposition of the Marrait and Tasiussaq moraine systems throughout the Disko Bugt region strongly suggests that regional climate variability forced changes in ice-sheet mass balance and acted as the primary trigger for early Holocene advances (or stillstands) of the western GrIS margin. We speculate that the Fjord Stade moraines, traceable along ~650 km of the southwestern GrIS, demarcate the widespread response of a significant portion of the GrIS during the 9.3 and 8.2 ka events (Alley et al., 1997; Rasmussen et al., 2007; Fleitmann et al., 2008).

In Greenland ice cores, the 9.3 and 8.2 ka events are defined by abrupt $\delta^{18}O$ excursions and are two of the most prominent abrupt climatic excursions after the Younger Dryas (Alley et al., 1997; Rasmussen et al., 2007; Thomas et al., 2007). The 9.3 and 8.2 ka events were likely triggered by freshwater outbursts of Laurentide Ice Sheet-dammed lakes into the North Atlantic Ocean and attendant changes in thermohaline circulation (Barber et al., 1999; Yu et al., 2010). The ~150-yr long 8.2 ka event was characterized by peak cooling of 3.3 ± 1.1 °C, whereas the 9.3 ka event was similar in amplitude, but shorter in duration (Kobashi et al., 2007; Rasmussen et al., 2007; Thomas et al., 2007). Thus, compared to millennial-scale abrupt climate oscillations of the last glacial period with large-amplitude temperature swings (e.g. the Younger Dryas, ~15 °C; Alley et al., 1993), the 9.3 and 8.2 ka events were extremely short-lived and of relatively small amplitude. Nonetheless, it appears that cooling during the 9.3 and 8.2 ka events was able to trigger a response of the western GrIS.

The suggestion that the deposition of the Fjord Stade moraines was due to the interaction between ice dynamics and topography, and decoupled from regional climate trends, relies on the asynchronous timing of moraine deposition across Disko Bugt (Long et al., 2006; Weidick and Bennike, 2007). At the Nuuk peninsula, basal lake sediment ^{14}C ages originally limited deposition of the Tasiussaq moraine to ~8.5–7.8 ka (Long and Roberts, 2002; see Section 5.2 above), while at Jakobshavn Isfjord, deposition of the Tasiussaq moraine was thought to have occurred before ~8.8 ka (Long et al., 2006). However, new ^{10}Be and ^{14}C ages, and a re-examination of existing chronological control, suggests otherwise. The ~8.8 ka basal lake sediment ^{14}C age from Jakobshavn Isfjord (Table 2; see Section 5.1 above) slightly inboard of the Tasiussaq moraine appears to be the lone ^{14}C or ^{10}Be age that does not support the ~8.2–8.0 ka age of the Tasiussaq moraine. Thus, we suggest that the 8.8 ka age is an outlier, perhaps influenced by old carbon contained within bulk sediments. In addition, we wonder if Disko Bugt's complex geomorphology and the generalized 'Fjord Stade moraines' label lead to added uncertainty surrounding the Fjord Stade moraines' chronology. For example, in some regions (e.g. Jakobshavn Isfjord) the Marrait and Tasiussaq moraines are closely nested and without direct age control, these moraines could be considered contemporaneous. Moreover, comparing ^{14}C or ^{10}Be ages that are associated with the generalized Fjord Stade moraines to other age constraints that relate directly to either the Marrait or Tasiussaq moraine is challenging and may give the appearance of asynchronous moraine deposition across different locations. In this regard, associating chronological constraints to specific Marrait- or Tasiussaq-related ice-margin deposits is paramount.

6.2. The Greenland Ice Sheet and early Holocene abrupt climate change

Records from the Northern Hemisphere suggest that glaciers in several regions may have advanced in response to the 8.2 ka event (Alley and Ágústdóttir, 2005). For example, the Finse Event may record a widespread 8.2 ka-event-driven advance of Scandinavian mountain glaciers (Nesje and Dahl, 2001), and glaciers in coastal Alaska and Canada may have also advanced in response to the 8.2 ka event (Denton and Karlén, 1973; Menounos et al., 2004). Continuous proxy records from the Northern Hemisphere provide widespread evidence for climatic anomalies associated with the 9.3 ka event (Fleitmann et al., 2008), but we are unaware of any records that capture a distinct glacier advance in response to the 9.3 ka cooling event. Glacier records of the 8.2 ka event are derived from independent mountain glacier systems, which are capable of responding quickly to climate perturbations (e.g. Oerlemans, 2005).

The western GrIS response to sub-centennial scale cooling events in the early Holocene indicates that the GrIS is capable of responding to short-lived climate change with lag times perhaps similar to those of mountain glacier systems. A key consideration is that abrupt cooling 9.3 and 8.2 ka interrupted an overall period of warmth, likely warmer than today (Dahl-Jensen et al., 1998; Kaufman et al., 2004; Vinther et al., 2009), during which time the western GrIS was rapidly retreating (Long and Roberts, 2003). The western GrIS margin was retreating prior to the 9.3 ka event and then advanced/paused in response to 9.3 ka event cooling. In a similar fashion, following retreat after the 9.3 ka event, the western GrIS margin advanced again in response to 8.2 ka event cooling and then proceeded to retreat under warmer-than-present conditions (Young et al., 2011a, 2011b), indicating that the western

GrIS margin fluctuated in lockstep with early Holocene temperature oscillations. Accordingly, post-8.2 ka event retreat of the western GrIS margin was driven by temperatures that were as much as 2 °C warmer than today in the west-central Greenland region, with marine ice margins likely influenced by the incursion of the warm West Greenland Current into eastern Disko Bugt ca 7.8 ka (Dahl-Jensen et al., 1998; Lloyd et al., 2005; Young et al., 2011a). The continued deglaciation and minimum extent of the western GrIS margin during the middle Holocene (e.g. Briner et al., 2010) were likely not a delayed response to warming at the last glacial termination, but rather reflects ice-margin coupling with early and middle Holocene summer temperature.

6.3. Magnitude of ice-margin response

Although our ice-margin chronology indicates that the western GrIS margin responded to the 9.3 and 8.2 ka events, geomorphic and chronological evidence suggests that the magnitude of ice-margin response resulting in deposition of the Marrait and Tasiussaq moraines differed between southeastern Disko Bugt and Jakobshavn Isfjord. On the Nuuk peninsula, ^{10}Be ages become progressively younger from west to east across three distinct morphostratigraphic surfaces: outboard of the Marrait moraine, between the Marrait and Tasiussaq moraines and inboard of the Tasiussaq ice limit (Figs. 3 and 7). Outboard of the Marrait moraine two ^{10}Be ages are ~9.4 ka, between the Marrait and Tasiussaq moraines ^{10}Be ages range from 9.1 to 8.4 ka, and inboard of the Tasiussaq moraine ^{10}Be ages range from ~8.3 to 7.9 ka. The ^{10}Be age distribution on the Nuuk peninsula, which tracks the ice-margin position almost continuously between ~9.4 ka and 7.9 ka, suggests that the Marrait and Tasiussaq moraines represent stillstands, or perhaps minor re-advances of the ice margin during gradual deglaciation (Fig. 7). Here, ^{10}Be ages directly outboard and inboard of each moraine are closely limiting maximum and minimum age constraints, respectively (Figs. 7 and 8).

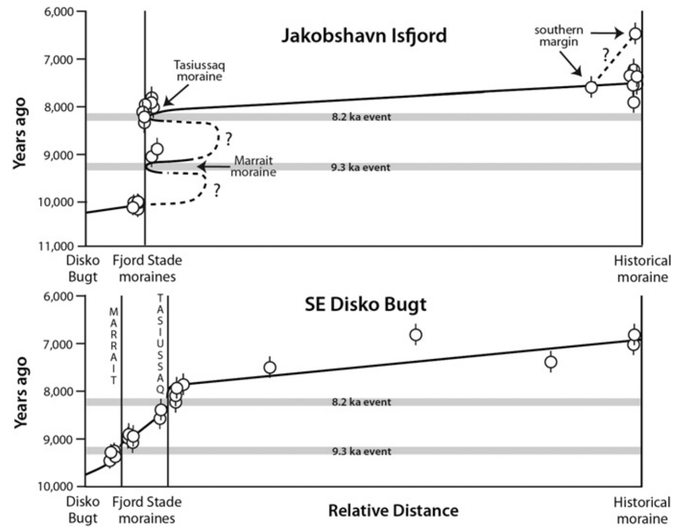

Fig. 8. ^{10}Be-based time–distance diagrams for the GrIS margin at Jakobshavn Isfjord and southeastern Disko Bugt. Each ^{10}Be age is shown with its corresponding 1σ uncertainty (bars). Southern margin – the two most southern ^{10}Be ages from Jakobshavn Isfjord near the current ice margin. It is unclear if the youngest age (6.5 ± 0.2 ka) is an outlier or instead reflects the delayed deglaciation of the ice-margin immediately south of Jakobshavn Isfjord.

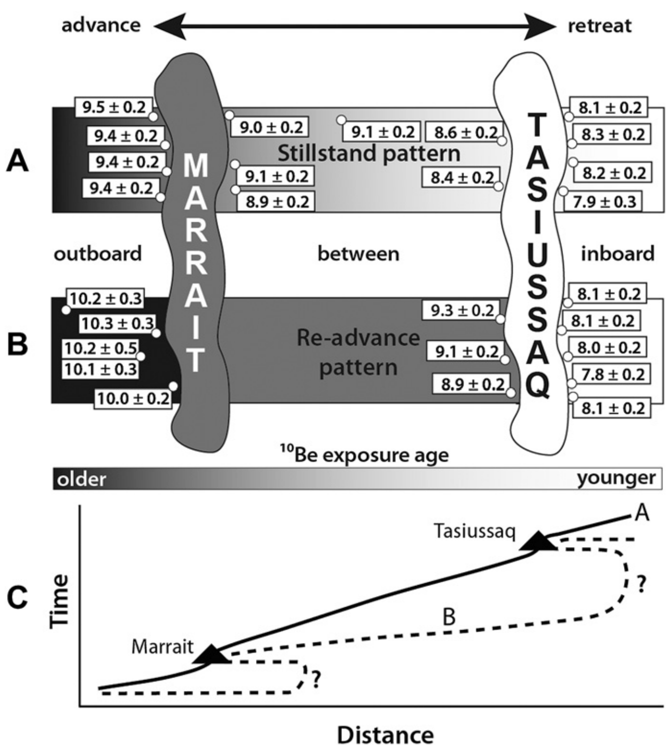

Fig. 7. Predicted distribution of ^{10}Be ages (shading) at locations where the Marrait and Tasiussaq moraines were deposited during stillstands versus at the culminations of re-advances. In scenario A, predicted ^{10}Be ages become progressively younger across three morphostratigraphic surfaces: 1) outboard of the Marrait moraine, 2) between moraines, and 3) inboard of the Tasiussaq. In this scenario, hypothetical ^{10}Be ages from directly outboard and inboard of the moraines closely bracket the timing of moraine deposition. In scenario B, the ice margin initially retreated an unknown distance inland of the Marrait moraine, before re-advancing to deposit the Marrait moraine. Following deposition of the Marrait moraine, the ice margin again retreated before re-advancing to deposit the Tasiussaq moraine. In both scenarios, hypothetical ^{10}Be ages from inboard of each moraine are close minimum constraints on the age of that moraine; however, only in the stillstand scenario do ^{10}Be ages outboard of each moraine act as close maximum constraining ages for that moraine. For comparison, actual ^{10}Be ages, not including outliers, and their positions relative to the Marrait and Tasiussaq moraines from southeastern Disko Bugt (A) and Jakobshavn Isfjord (B) are also shown. (C) Time-distance diagram illustrating the behavior of an ice margin depositing the Marrait and Tasiussaq moraines via stillstands or re-advances.

At Jakobshavn Isfjord, on the other hand, the distribution of ^{10}Be ages across the Fjord Stade moraines differs. North of the fjord, where the Marrait and Tasiussaq moraines are separated (Figs. 2 and 5), ^{10}Be ages cluster into three groups and do not continuously track ice-margin position: outboard of the Marrait moraine ^{10}Be ages are between ~10.2 and 10.0 ka, between the two moraines ^{10}Be ages fall between ~9.3 and 8.9 ka, and inboard of the Tasiussaq moraine ^{10}Be ages are ~8.1–7.8 ka. The distribution of ^{10}Be ages at Jakobshavn Isfjord, combined with Pluto Lake's sediment stratigraphy and overlapping moraines up-fjord, indicates that the northern ice margin's behavior between ~10 and 8 ka was characterized by significant re-advances superposed upon deglaciation. In summary, Jakobshavn Isbræ experienced quick retreat during the early Holocene that was punctuated by re-advances ~9.2 and 8.2 ka (Young et al., 2011b), whereas the ice margin on the Nuuk peninsula likely experienced gradual retreat with stillstands or minor re-advances 9.4–9.0 and 8.5–8.1 ka (Figs. 7 and 8).

The difference in ice-margin response between Jakobshavn Isfjord and southeastern Disko Bugt may partly be explained by two glaciologically distinct ice-flow regimes. For example, a dichotomy is apparent when observing modern GrIS and Antarctic Ice Sheet change: marine-based margins display enhanced sensitivity (i.e. retreat and thinning) to regional warming compared to land-terminating margins, resulting from dynamically driven feedback mechanisms (De Angelis and Skvarca, 2003; Csatho et al., 2008). Jakobshavn Isbræ and other marine-terminating outlet glaciers are characterized by ice velocities on the order of km yr^{-1}, and ice-margin fluctuations are heavily influenced by ice dynamic and oceanographic processes operating at the terminus (Joughin et al., 2004; Rignot and Kanagaratnam, 2006; Holland et al., 2008; Briner et al., 2009; Rignot et al., 2010). In contrast, the southeastern Disko Bugt ice margin, more similar to the majority of the southwestern GrIS, was mostly land-terminating and likely flowed at significantly slower velocities, ultimately allowing it to be less susceptible to ice dynamic (e.g. iceberg calving) and oceanographic forcing. We suggest that ice-sheet margins with high ice fluxes display an exaggerated response to abrupt cooling due to much quicker response times than margins characterized by slower ice velocities. In high ice-flux sectors, a mass balance shift triggered by regional cooling (i.e. reduced summer ablation) would be transferred quickly to the margin resulting in ice-sheet advance. Alternatively, at low ice-flux sectors with slower response times, mass-balance change would be integrated over a longer period resulting in a muted response (i.e. stillstand) to cooling of the same magnitude. It is interesting that Jakobshavn Isbræ advanced to deposit both the Marrait and Tasiussaq moraines because calving glaciers' advance and retreat cycles can often function independently of climate (e.g. Trabant et al., 2003; Post et al., 2011). Advance of Jakobshavn Isbræ through its deep fjord was likely facilitated by rapid sedimentation at the glacier front (e.g. Nick et al., 2007), and perhaps influenced by increased sea-ice cover during the 9.3 and 8.2 ka events. Increased sea-ice cover may have stabilized the ice mélange in the Isfjord, resulting in reduced calving and therefore advance of the high-flux terminus in response to the 9.3 and 8.2 ka events (Amundson et al., 2010).

7. Conclusion

Our chronology of the western GrIS margin history merges new and preexisting ^{14}C and ^{10}Be ages from two regions to show that the Marrait and Tasiussaq moraines dispersed across Disko Bugt record the response of the western GrIS to the 9.3 and 8.2 ka cooling events. Jakobshavn Isbræ reversed a pattern of retreat twice in the early Holocene to deposit the Marrait and Tasiussaq moraines ~9.2 and 8.2–8.0 ka, respectively. The ice margin in southeastern Disko Bugt experienced two stillstands to deposit the Marrait and Tasiussaq moraines between ~9.4–9.0 and ~8.5–8.1 ka. Modern observations reveal that marine-terminating outlets exhibit a greater response to regional warming compared to adjacent land-terminating ice margins; our results suggest this relationship also applies to phases of ice-sheet expansion in the past. The long-term (i.e. millennial-scale) history of the GrIS clearly indicates that the GrIS shrinks in response to warming and grows during cooler periods (Alley et al., 2010), and based on our results, also does so on human (centennial) timescales. In addition, the response of the western GrIS to such short-lived climate excursions indicates that a long-term climatic trend is not needed to trigger a large-scale response from the ice sheet. The lock-step response of the western GrIS to climate change is consistent with ice-sheet models that routinely depict western GrIS margins experiencing a larger response to climate change than other regions of the GrIS (Tarasov and Peltier, 2003; Alley et al., 2005; Simpson et al., 2009). Whether other sectors of the GrIS are able to respond quickly to abrupt climate change remains an open question.

These data highlight how the link between climate, ice dynamics and ice-sheet behavior, and at what timescales these forcing mechanisms operate, can be better understood by generating paleo-records of ice-margin change. Additional data from other regions fringing the GrIS, however, are needed to indentify the mechanisms driving ice-sheet fluctuations on decadal to centennial timescales. This precise chronology of western GrIS margin change provides important benchmarks for ice-sheet modelers striving to predict the future response of the GrIS to climate change.

Acknowledgments

We thank Kurt Kjær for kindly providing air photographs and CH2M Hill for logistical support. We also thank Sam Kelley, Elizabeth Thomas and Stefan Truex for assistance in the field and laboratory. Reviews from Vincent Rinterknecht and an anonymous reviewer improved this manuscript. This work was supported by the U.S. National Science Foundation Geography and Spatial Sciences Program (NSF-BCS 0752848 and NSF-BCS 1002597).

References

Alley, R.B., Áugústdóttir, A.M., 2005. The 8k event: cause and con-sequences of a major Holocene abrupt climate change. Quaternary Science Reviews 24, 1123–1149.
Alley, R.B., Meese, D.A., Shuman, C.A., Gow, A.J., Taylor, K.C., Grootes, P.M., White, J.W.C., Ram, M., Waddington, E.D., Mayewski, P.A., Zielinski, G.A., 1993. Abrupt increase in snow accumulation at the end of the Younger Dryas event. Nature 362, 527–529.
Alley, R.B., Mayewski, P.A., Sowers, T., Stuiver, M., Taylor, K.C., Clark, P.U., 1997. Holocene climatic instability: a prominent, widespread event 8200 yr ago. Geology 25, 483–486.
Alley, R.B., Clark, P.U., Huybrechts, P., Joughin, I., 2005. Ice-sheet and sea-level changes. Science 310, 456–460.
Alley, R., Andrews, J., Brigham-Grette, J., Clarke, G., Cuffey, K., Fitzpatrick, J., Funder, S., Marshall, S., Miller, G., Mitrovica, J., 2010. History of the Greenland ice sheet: paleoclimatic insights. Quaternary Science Reviews 29, 1728–1756.
Amundson, J.M., Fahnestock, M., Truffer, M., Brown, J., Lüthi, M.P., Motyka, R.J., 2010. Ice mélange dynamics and implications for terminus stability, Jakobshavn Isbræ, Greenland. Journal of Geophysical Research 115, F01005.
Balco, G., Stone, J.O., Lifton, N.A., Dunai, T.J., 2008. A complete and easily accessible means of calculating surface exposure ages or erosion rates from ^{10}Be and ^{26}Al measurements. Quaternary Geochronology 3, 174–195.
Balco, G., Briner, J., Finkel, R.C., Rayburn, J.A., Ridge, J.C., Schaefer, J.M., 2009. Regional beryllium-10 production rate calibration for northeastern North America. Quaternary Geochronology 4, 93–107.
Barber, D.C., Dyke, A., Hillaire-Marcel, C., Jennings, A.E., Andrews, J.T., Kerwin, M.W., Bilodeau, G., McNeely, R., Southon, J., Morehead, M.D., Gagnon, J.M., 1999. Forcing of the cold event of 8,200 years ago by catastrophic drainage of Laurentide lakes. Nature 400, 344–348.
Bennike, O., Bjorck, S., 2002. Chronology of the last recession of the Greenland ice sheet. Journal of Quaternary Science 17, 211–219.
Bennike, O., Anderson, N.J., McGowan, S., 2010. Holocene palaeoecology of southwest Greenland inferred from macrofossils in sediments of an oligosaline lake. Journal of Paleolimnology 43, 787–798.
Briner, J.P., Bini, A.C., Anderson, R.S., 2009. Rapid early Holocene retreat of a Laurentide outlet glacier through an Arctic fjord. Nature Geoscience 2, 496–499.
Briner, J.P., Stewart, H.A.M., Young, N.E., Phillips, W., Losee, S., 2010. Using proglacial-threshold lakes to constrain fluctuations of the Jakobshavn Isbræ ice margin, western Greenland, during the Holocene. Quaternary Science Reviews 29, 3861–3874.
Briner, J.P., Young, N.E., Goehring, B.M., Schaefer, J.M., 2012. Constraining ^{10}Be production rates on Greenland. Journal of Quaternary Science 27, 2–6.
Corbett, L.B., Young, N.E., Bierman, P.R., Briner, J.P., Neumann, T.A., Rood, D.H., Graly, J.A., 2011. Paired bedrock and boulder ^{10}Be concentrations resulting from early Holocene ice retreat near Jakobshavn Isfjord. Quaternary Science Reviews 30, 1739–1749.
Coulthard, R.D., Furze, M.F.A., Pienkowski, A.J., Chantel Nixon, F., England, J.H., 2010. New marine ΔR values for Arctic Canada. Quaternary Geochronology 5, 419–434.
Csatho, B., Schenk, T., van der Veen, C.J., Krabill, W.B., 2008. Intermittent thinning of Jakobshavn Isbræ, west Greenland. Journal of Glaciology 54, 131–144.
Dahl-Jensen, D., Mosegaard, K., Gundestrup, N., Clow, G.D., Johnsen, S.J., Hansen, A.W., Balling, N., 1998. Past temperatures directly from the Greenland Ice Sheet. Science 282, 268–271.
De Angelis, H., Skvarca, P., 2003. Glacier surge after ice shelf collapse. Science 299, 1560–1562.
Denton, G.H., Karlén, W., 1973. Holocene climate variations—their pattern and possible cause. Quaternary Research 3, 155–205.
Donner, J., Junger, H., 1975. Radiocarbon dating of shells from marine Holocene deposits in the Disko Bugt area, West Greenland. Boreas 4, 25–45.

Fleitmann, D., Mudelsee, M., Burns, S.J., Bradley, R.S., Kramers, J., Matter, A., 2008. Evidence for a widespread climatic anomaly at around 9.2 ka before present. Paleoceanography 23, PA1102.

Funder, S., Kjeldsen, K.K., Kjær, K.H., Cofaigh, C.Ó, 2011. The Greenland Ice Sheet during the past 300,000 years: a review. In: Ehlers, J., Gibbard, P.L. (Eds.), Quaternary Glaciations: Extent and Chronology, Developments in Quaternary Science, vol. 2. Elsevier, Amsterdam, pp. 699–713.

Garde, A.A., Steenfelt, A., 1999. Precambrian geology of Nuussuaq and the area north-east of Disko Island. In: Kalsbeek, F. (Ed.), Precambrian Geology of the Disko Bugt Region, West Greenland. Geology of Greenland Survey Bulletin 181, pp. 6–40.

Gosse, J.C., Phillips, F.M., 2001. Terrestrial in situ cosmogenic nuclides: theory and application. Quaternary Science Reviews 20, 1475–1560.

Holland, D.M., Thomas, R.H., de Young, B., Ribergaard, M.H., Lyberth, B., 2008. Acceleration of Jakobshavn Isbræ triggered by warm subsurface ocean waters. Nature Geoscience 1, 659–664.

Howat, I.M., Joughin, I., Scambos, T.A., 2007. Rapid changes in ice discharge from Greenland outlet glaciers. Science 315, 1559–1561.

Ingólfsson, Ó, Frich, P., Funder, S., Humlum, O., 1990. Paleoclimatic implications of an early Holocene glacier advance on Disko Island, west Greenland. Boreas 19, 297–311.

Joughin, I., Abdalati, W., Fahnestock, M., 2004. Large fluctuations in speed on Greenland's Jakobshavn Isbræ glacier. Nature 432, 608–610.

Kaplan, M.R., Wolfe, A.P., Miller, G.H., 2002. Holocene environmental variability in southern Greenland inferred from lake sediments. Quaternary Research 58, 149–159.

Kaufman, D.S., Ager, T.A., Anderson, N.J., Anderson, P.M., Andrews, J.T., Bartlein, P.J., Brubaker, L.B., Coats, L.L., Cwynar, L.C., Duvall, M.L., Dyke, A.S., Edwards, M.E., Eisner, W.R., Gajewski, K., Geirsdóttir, A., Hu, F.S., Jennings, A.E., Kaplan, M.R., Kerwin, M.W., Lozhkin, A.V., MacDonald, G.M., Miller, G.H., Mock, C.J., Oswald, W.W., Otto-Bliesner, B.L., Pornichu, D.F., Ruhland, K., Smol, J.P., Steig, E.J., Wolfe, B.B., 2004. Holocene thermal maximum in the western Arctic (0–180° W). Quaternary Science Reviews 23, 529–560.

Kelly, M.A., Lowell, T.V., 2009. Fluctuations of local glaciers in Greenland during latest Pleistocene and Holocene time. Quaternary Science Reviews 28, 2088–2106.

Kelly, M., 1985. A review of the Quaternary geology of western Greenland. In: Andrews, J.T. (Ed.), Quaternary Environments; Eastern Canadian Arctic, Baffin Bay and Western Greenland. Alien and Unwin, Boston, pp. 461–501.

Kobashi, T., Severinghaus, J.P., Brook, E.J., Barnola, J.M., Grachev, A.M., 2007. Precise timing and characterization of abrupt climate change 8200 years ago from air trapped in polar ice. Quaternary Science Reviews 26, 1212–1222.

Kohl, C., Nishiizumi, K., 1992. Chemical isolation of quartz for measurement of in-situ- produced cosmogenic nuclides. Geochimica et Cosmochimica Acta 56, 3583–3587.

Lal, D., 1991. Cosmic ray labeling of erosion surfaces: *in situ* nuclide production rates and erosion models. Earth and Planetary Science Letters 104, 424–439.

Lloyd, J.M., Park, L.A., Kuijpers, A., Moros, M., 2005. Early Holocene paleoceanography and deglacial chronology of Disko Bugt, west Greenland. Quaternary Science Reviews 24, 1741–1755.

Long, A.J., Roberts, D.H., 2002. A revised chronology for the 'Fjord Stade' moraine in Disko Bugt, west Greenland. Journal of Quaternary Science 17, 561–579.

Long, A.J., Roberts, D.H., 2003. Late Weichselian deglacial history of Disko Bugt, West Greenland, and the dynamics of Jakobshavns Isbræ ice stream. Boreas 32, 208–226.

Long, A.J., Roberts, D.H., Rasch, M., 2003. New observations on the relative sea level and deglacial history of Greenland from Innaarsuit, Disko Bugt. Quaternary Research 60, 162–171.

Long, A.J., Roberts, D.H., Dawson, S., 2006. Early Holocene history of the west Greenland Ice Sheet and the GH-8.2 event. Quaternary Science Reviews 25, 904–922.

Long, A.J., Woodroffe, S.A., Roberts, D.H., Dawson, S., 2011. Isolation basins, sea-level changes and the Holocene history of the Greenland Ice Sheet. Quaternary Science Reviews 30, 3748–3768.

McGowan, S., Ryves, D.B., Anderson, N.J., 2003. Holocene records of effective precipitation in West Greenland. The Holocene 13, 239–249.

McNeely, R., Dyke, A.S., Southon, J.R., 2006. Canadian Marine Reservoir Ages, Preliminary Data Assessment. Open File 5049. Geological Survey of Canada, 3 pp.

Menounos, B., Koch, J., Osborn, G., Clague, J.J., Mazzuchi, D., 2004. Early Holocene glacier advance, southern coast mountains, British Colombia, Canada. Quaternary Science Reviews 23, 1543–1550.

Nesje, A., Dahl, S.O., 2001. The Greenland 8200 cal. yr BP event detected in loss-on-ignition profiles in Norwegian lacustrine sediment sequences. Journal of Quaternary Science 16, 155–166.

Nick, F.M., van der Veen, C.J., Oerlemans, J., 2007. Controls on advance of tidewater glaciers: results from numerical modeling applied to Columbia Glacier. Journal of Geophysical Research 112, F03S24. http://dx.doi.org/10.1029/2006JF000551.

Nishiizumi, K., Imamura, M., Caffee, M., Southon, J., Finkel, R., McAninch, J., 2007. Absolute calibration of ^{10}Be AMS standards. Nuclear Instruments and Methods in Physics Research Section B: Beam Interactions with Materials and Atoms 258, 403–413.

Oerlemans, J., 2005. Extracting a climate signal from 169 glacier records. Science 308, 675–677.

Otto-Bliesner, B.L., Marshall, S.J., Overpeck, J.T., Miller, G.H., Hu, A., Last Interglacial Project Members, C.A.P.E., 2006. Simulating polar amplification of orbital forcing for the Last Interglacial. Science 311, 1751–1753.

Pfeffer, W.T., Harper, J.T., O'Neel, S., 2008. Kinematic constraints on glacier contributions to 21st-century sea-level rise. Science 321, 1340–1343.

Post, A., O'Neel, S., Motyka, R.J., Streveler, G., 2011. A complex relationship between calving glaciers and climate. Eos, Transactions, American Geophysical Union 92.

Rasmussen, S.O., Vinther, B.O., Clausen, H.B., Andersen, K.K., 2007. Early Holocene climate oscillations recorded in three Greenland ice cores. Quaternary Science Reviews 26, 1907–1914.

Rignot, E., Kanagaratnam, P., 2006. Changes in the velocity structure of the Greenland ice sheet. Science 311, 986–990.

Rignot, E., Koppes, M., Velicogna, I., 2010. Rapid submarine melting of the calving faces of west Greenland glaciers. Nature Geoscience 3, 187–191.

Rood, D.H., Hall, S., Guilderson, T.P., Finkel, R.C., Brown, T.A., 2010. Challenges and opportunities in high precision Be-10 measurements at CAMS. Nuclear Instruments and Methods B: Beam Interactions with Material and Atoms 268, 730–732.

Simpson, M.J.R., Milne, G.A., Huybrechts, P., Long, A.J., 2009. Calibrating a glaciological model of the Greenland ice sheet from the last glacial maximum to present-day using field observations of relative sea level and ice extent. Quaternary Science Reviews 28, 1631–1657.

Stone, J.O., 2000. Air pressure and cosmogenic isotope production. Journal of Geophysical Research 105, 23,753–23,759.

Stuiver, M., Reimer, P.J., Reimer, R.W., 2005. CALIB 5.0. http://calib.qub.ac.uk/calib/.

Tarasov, L., Peltier, W.R., 2003. Greenland glacial history, borehole constraints, and Eemian extent. Journal of Geophysical Research 108, 2143. http://dx.doi.org/10.1029/20 01JB0 01731.

Tauber, H., 1968. Copenhagen radiocarbon dates IX. Radiocarbon 10, 295–327.

Ten Brink, N.W., Weidick, A., 1974. Greenland ice sheet history since the last glaciation. Quaternary Research 4, 429–440.

Thomas, E.R., Wolff, E.W., Mulvaney, R., Steffensen, J.P., Johnsen, S.J., Arrowsmith, C., White, J.W.C., Vaughn, B., Popp, T., 2007. The 8.2 ka event from Greenland ice cores. Quaternary Science Reviews 26, 70–81.

Trabant, D.C., Krimmel, R.M., Echelmeyer, K.A., Zirnheld, S.L., Elsberg, D.H., 2003. The slow advance of a calving glacier: Hubbard Glacier, Alaska, U.S.A. Annals of Glaciology 36, 45–50.

van den Broeke, M., Bamber, J., Ettema, J., Rignot, E., Schrama, E., van de Berg, W.J., van Meijgaard, E., Velicogna, I., Wouters, B., 2009. Partioning recent Greenland mass loss. Science 326, 984–986.

Vinther, B., Buchardt, S., Clausen, H., Dahl-Jensen, D., Johnsen, S., Fisher, D., Koerner, R., Raynaud, D., Lipenkov, V., Andersen, K., 2009. Holocene thinning of the Greenland ice sheet. Nature 461, 385–388.

Warren, C.R., Hulton, N.R.J., 1990. Topographic and glaciological controls on Holocene ice- sheet margin dynamics, central West Greenland. Annals of Glaciology 14, 307–310.

Weidick, A., Bennike, O., 2007. Quaternary glaciation history and glaciology of Jakobshavn Isbræ and the Disko Bugt region, West Greenland: a review. Geological Survey of Denmark and Greenland Bulletin 14, 1–78.

Weidick, A., 1968. Observations on some Holocene glacier fluctuations in West Greenland. Meddelelser om Grønland 165, 202.

Weidick, A., 1974. Quaternary Map of Greenland, Søndre Strømfjord – Nûgssuaq, 1: 500,000. Geological Survey of Greenland, Copenhagen.

Weidick, A., 1985. Review of glacier changes in West Greenland. Zeitschrift für Gletscherkunde und Glazialgeologie 21, 301–309.

Young, N.E., Briner, J.P., Stewart, H.A.M., Axford, Y., Csatho, B., Rood, D.H., Finkel, R.C., 2011a. Response of Jakobshavn Isbræ Greenland, to Holocene climate change. Geology 39, 131–134.

Young, N.E., Briner, J.P., Axford, Y., Csatho, B., Babonis, G.S., Rood, D.H., Finkel, R.C., 2011b. Response of a marine-terminating Greenland outlet glacier to abrupt cooling 8200 and 9300 years ago. Geophysical Research Letters 38, L24701.

Yu, S.H., Colman, S.M., Lowell, T.V., Milne, G.A., Fisher, T.G., Breckenridge, A., Boyd, M., Teller, J.T., 2010. Freshwater outburst from Lake Superior as a trigger for the cold event 9300 years ago. Science 328, 1262–1266.